The Galactic Center : Past and Future - 1

Cologne-Prague-Brno meeting 2022
Black-hole activity feedback from Bondi-radius
to galaxy-cluster scales
2022 June 1-3, Brno, Czech Republic,

Andreas Eckart

I.Physikalisches Institut der Universität zu Köln
Max-Planck-Institut für Radioastronomie, Bonn

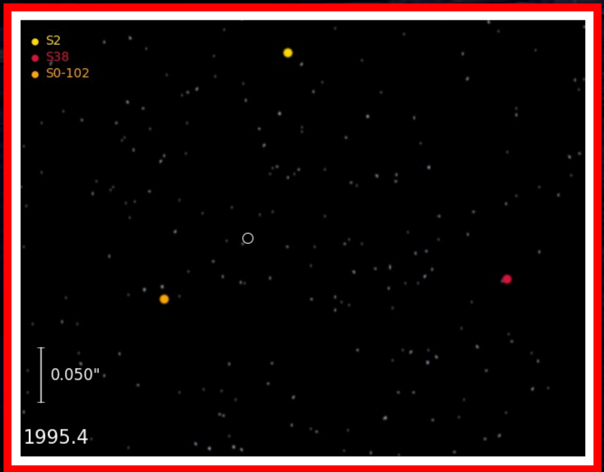

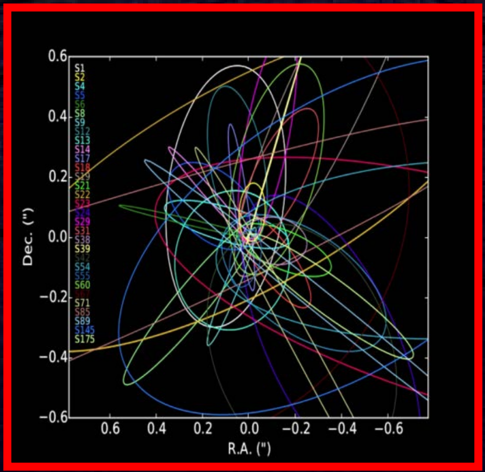

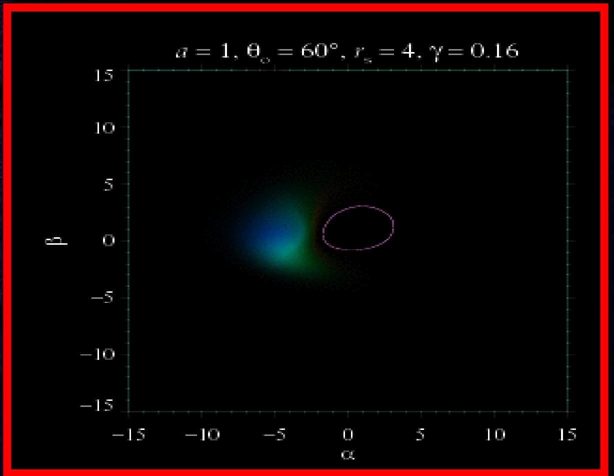

Why does one study super-compact masses?

Physics of extreme states of matter

No laboratory experiment possible (for massive black holes)

Test of the laws of physics in the high mass regime

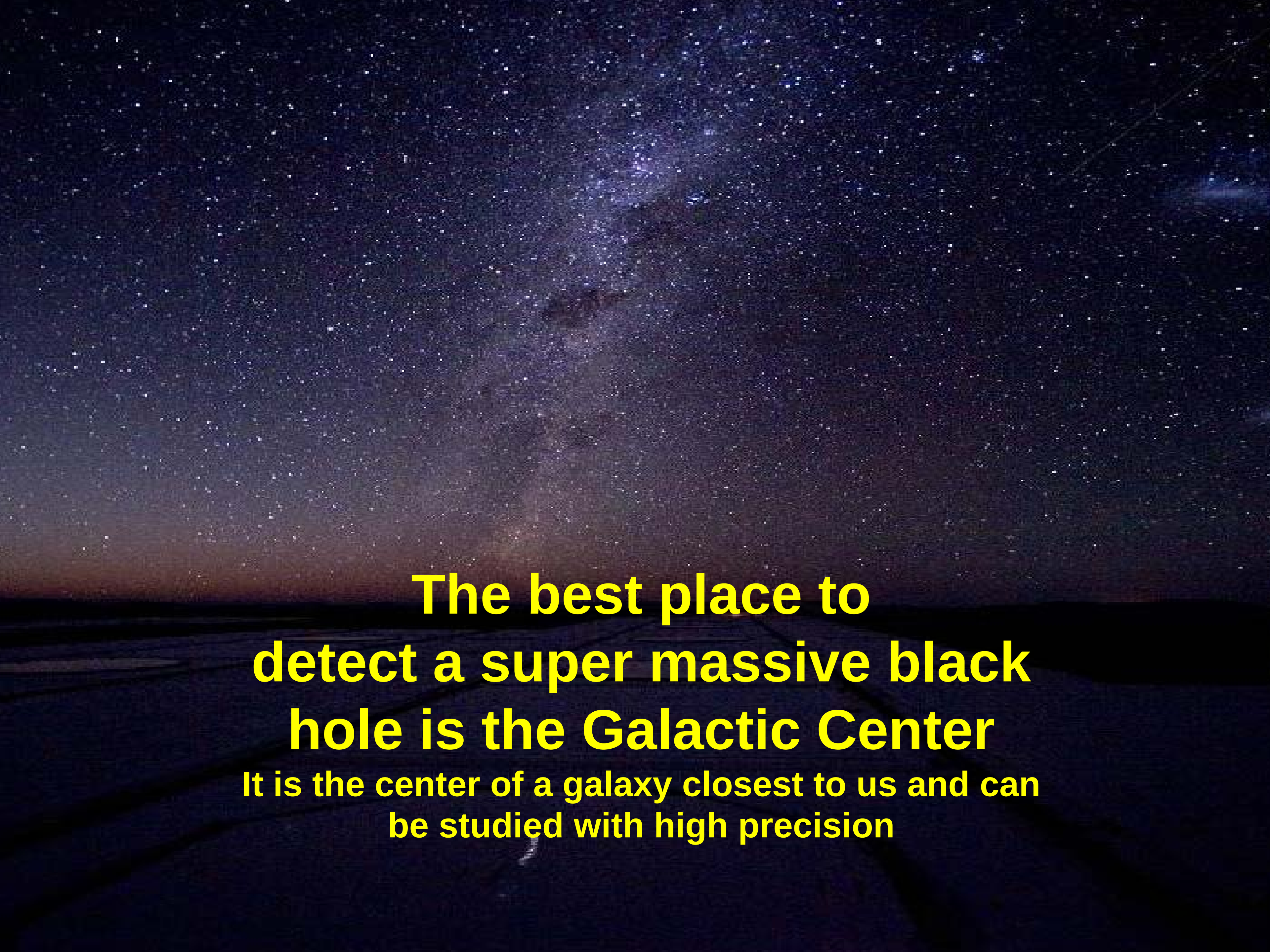

The best place to detect a super massive black hole is the Galactic Center

It is the center of a galaxy closest to us and can be studied with high precision

The Center of the Milky Way

Closest galactic nucleus
8 kpc distance
26.4000 lyrs
Extinction Av=30 Ak=3
Observations only in radio, infrared, X-ray

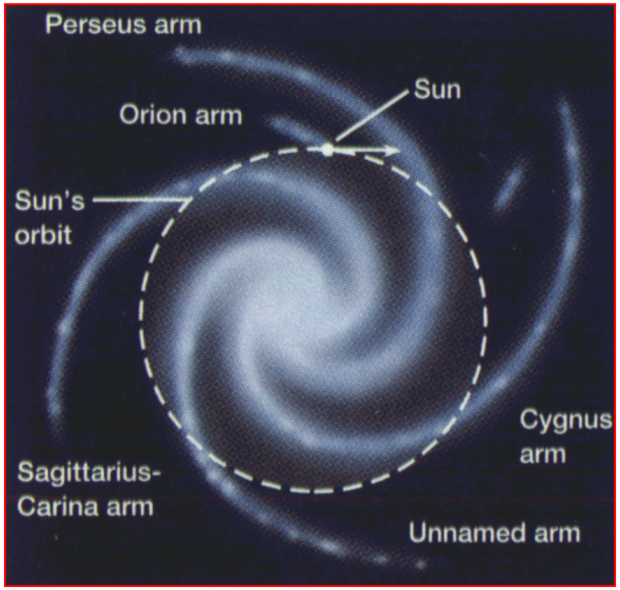

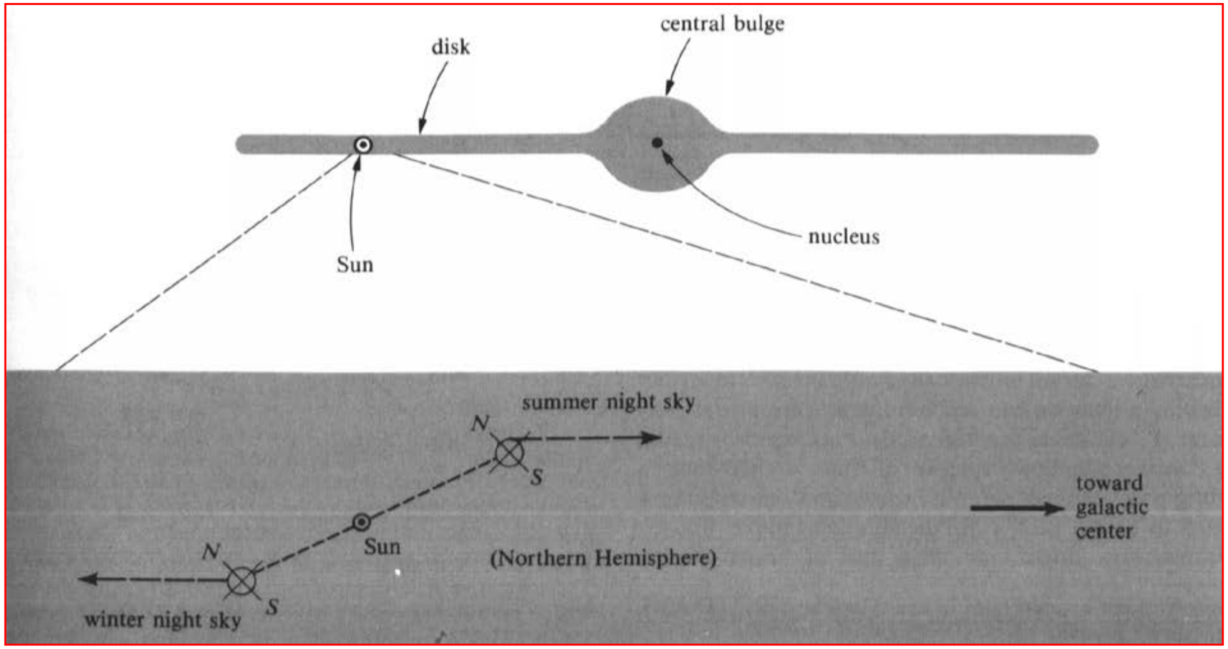

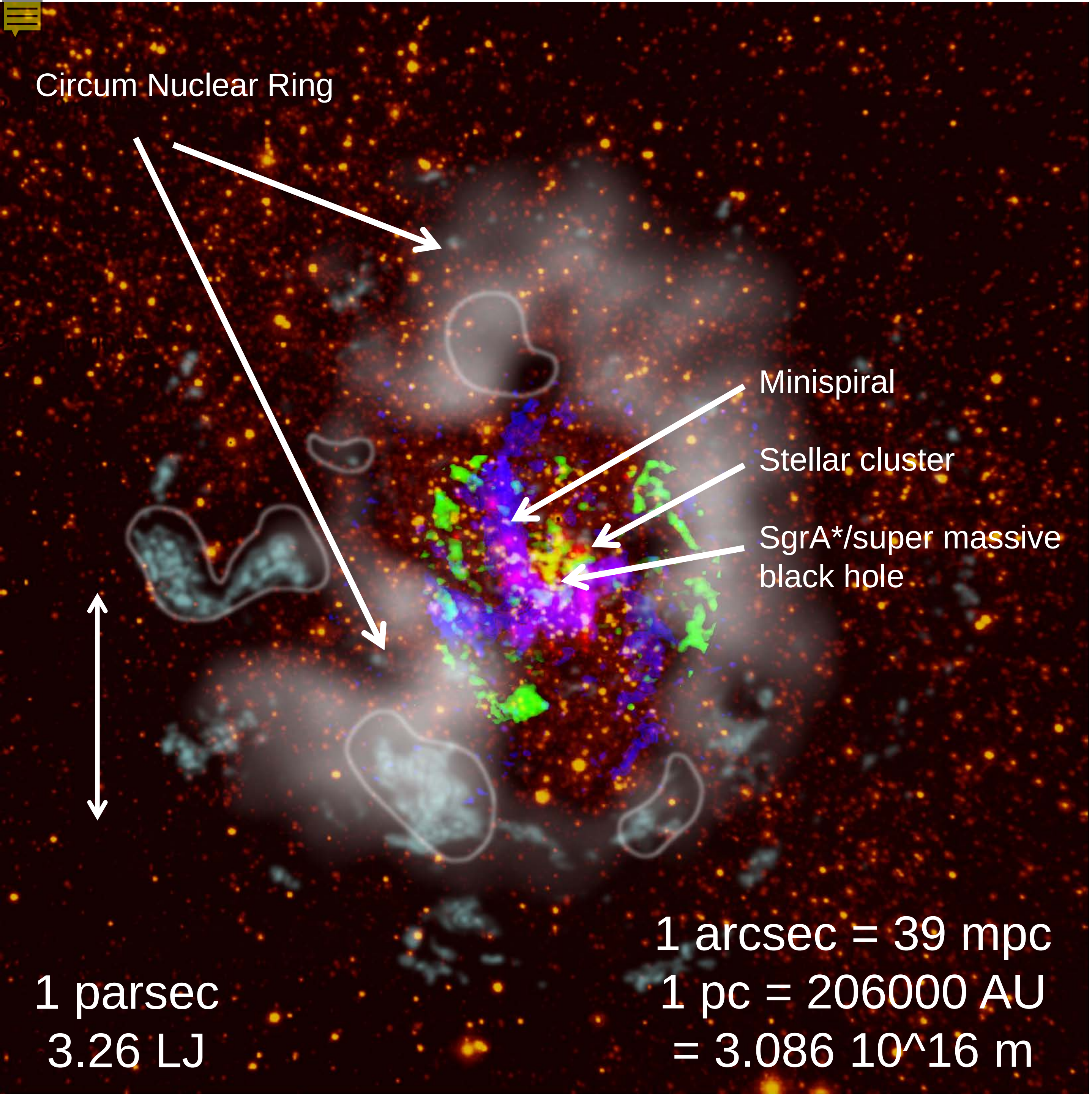

VLT infrared

ALMA submillimeter

Chandra X-ray

View of the Galactic Center

~1.5 arcmin across (11 light years)

Eckart et al. 2019 (UAE Sharjah - FISICPAC Proceeedings)

The Black Hole at the Center of the Milky Way
Eckart, Schödel, & C. Straubmeier 2005
Imperial College Press, London

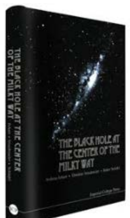

Past and Future Cosmologically

Past and Future Instrumentally

Past and Future Observationally

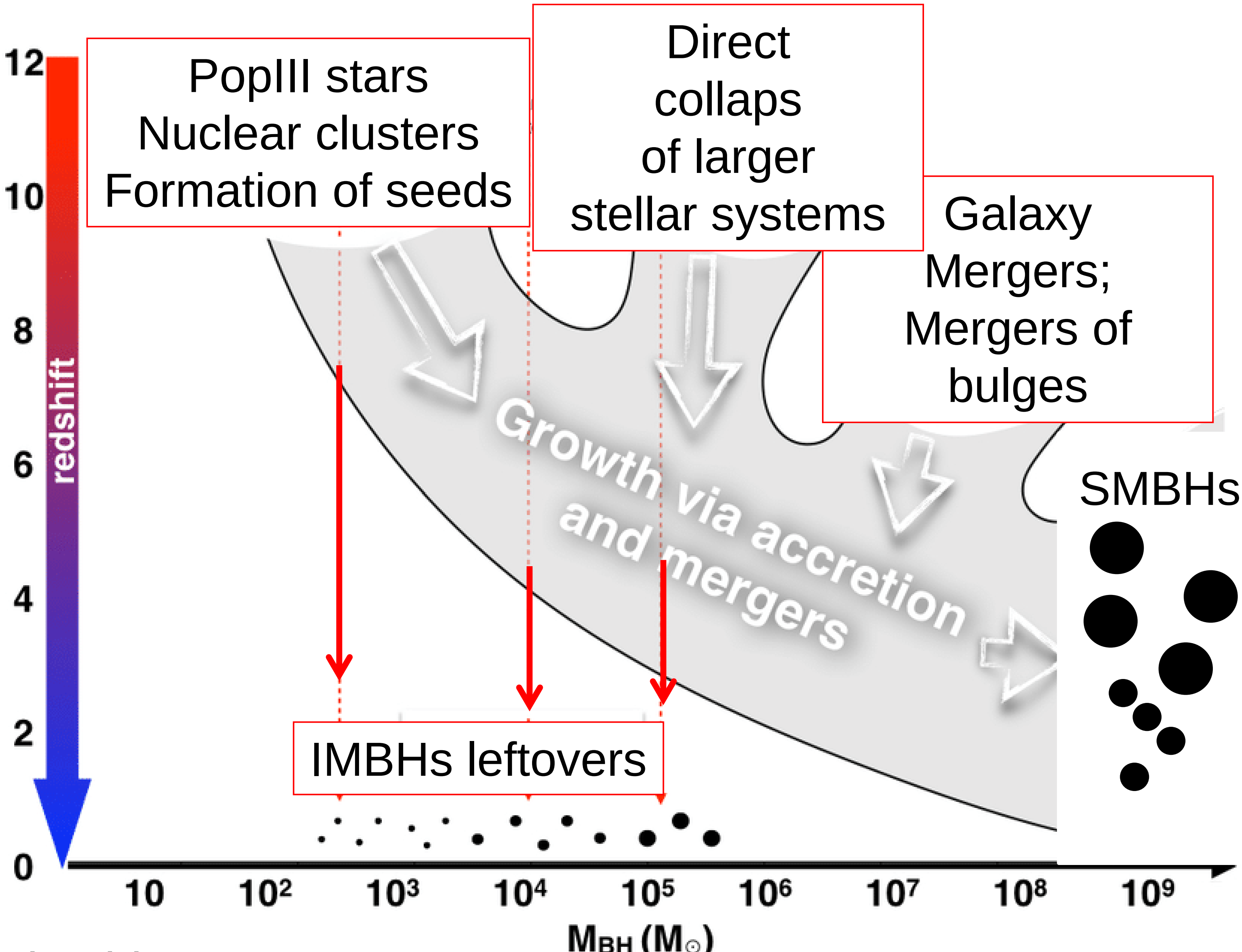

accretion history

Collision of Galaxies

Antennen-Galaxie
NGC 4038/39

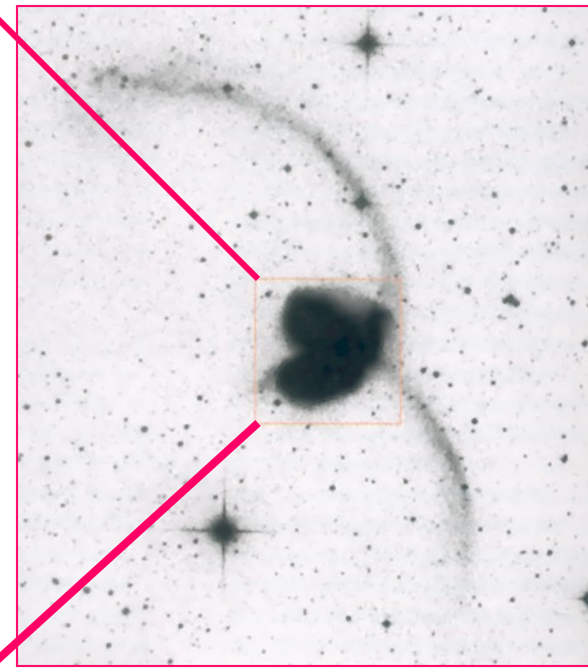

20 Mpc Entfernung
1“ = 140 pc

Aglomeration of BHs, stars, gas

Past and Future Cosmologically

Past and Future Instrumentally

Past and Future Observationally

NIR/MIR

Radio

The first 2.2μm scans through the GC

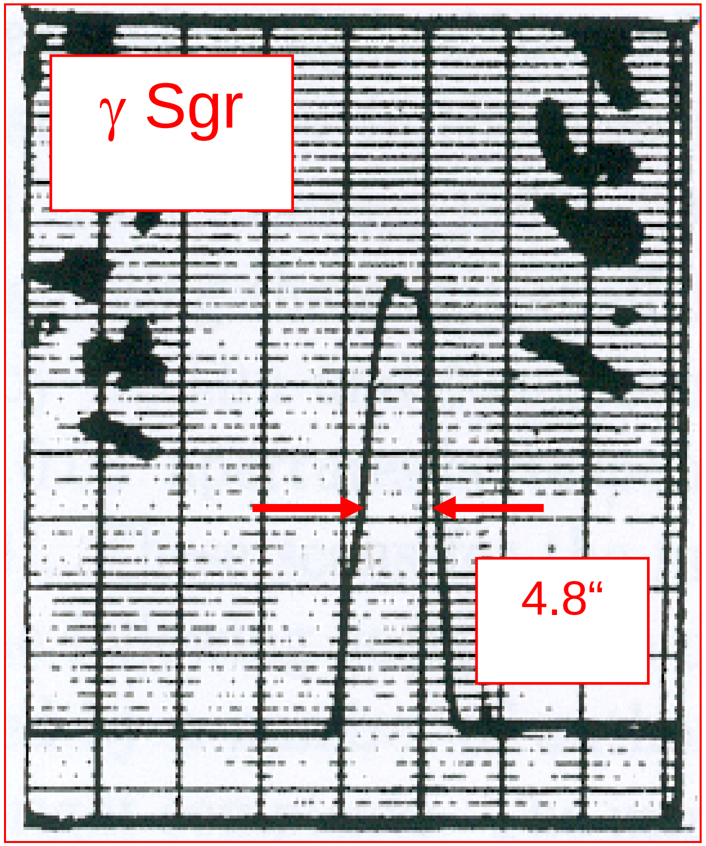

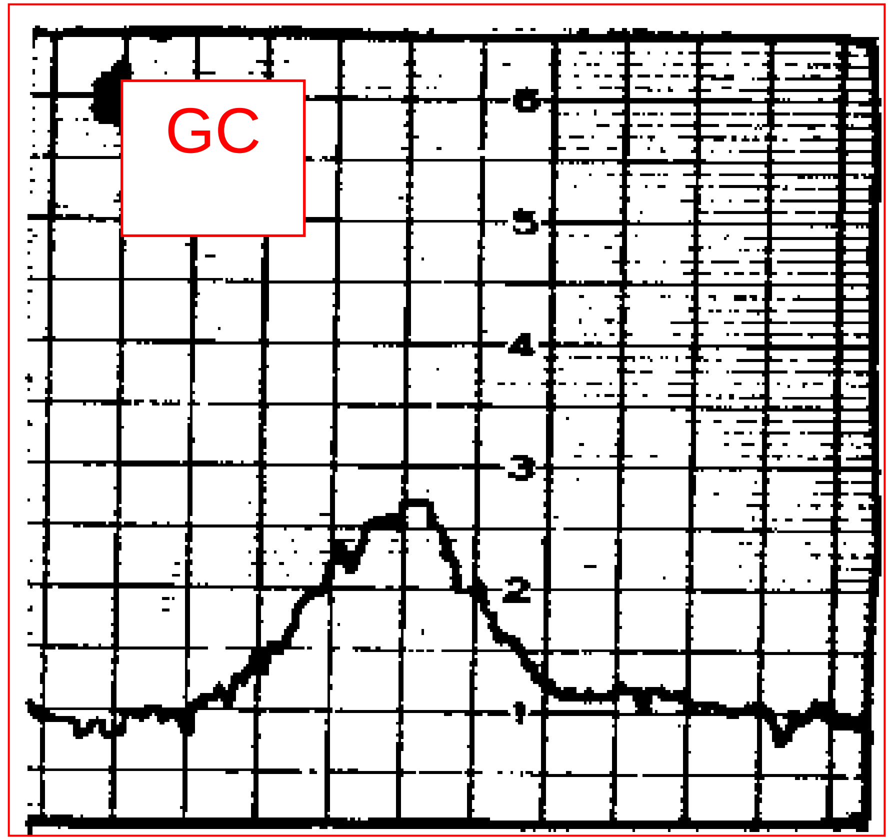

R.A. scans with a single pixel detector (Becklin & Naugebauer 1968)

The first 2.2µm scans through the GC

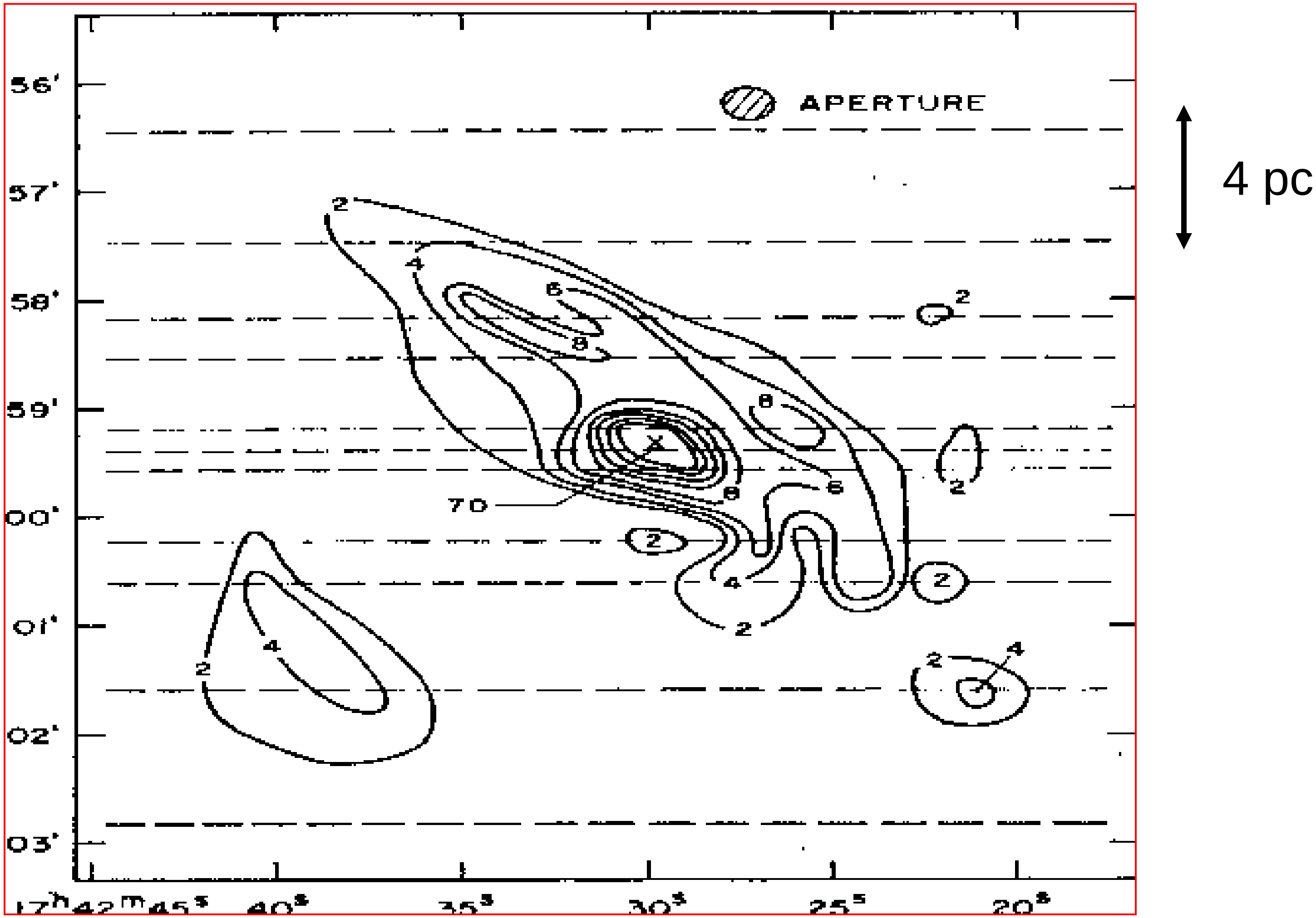

R.A. scans with a single pixel detector (Becklin & Naugebauer 1968)

The first 2.2µm scans through the GC

4 pc

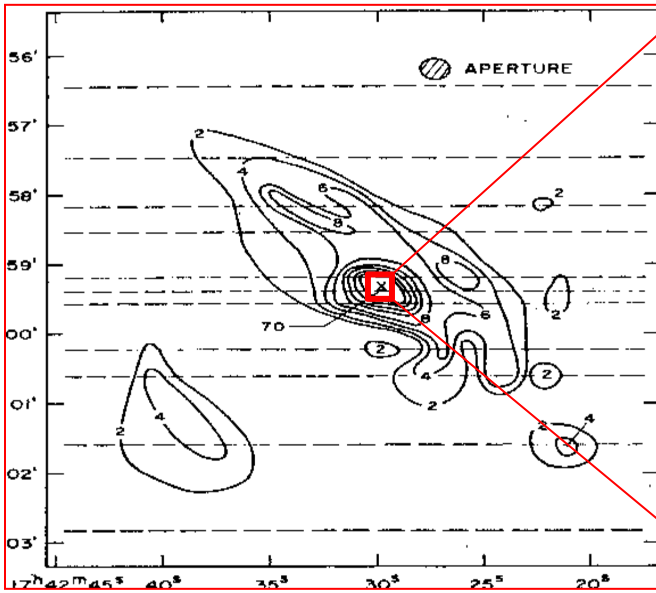

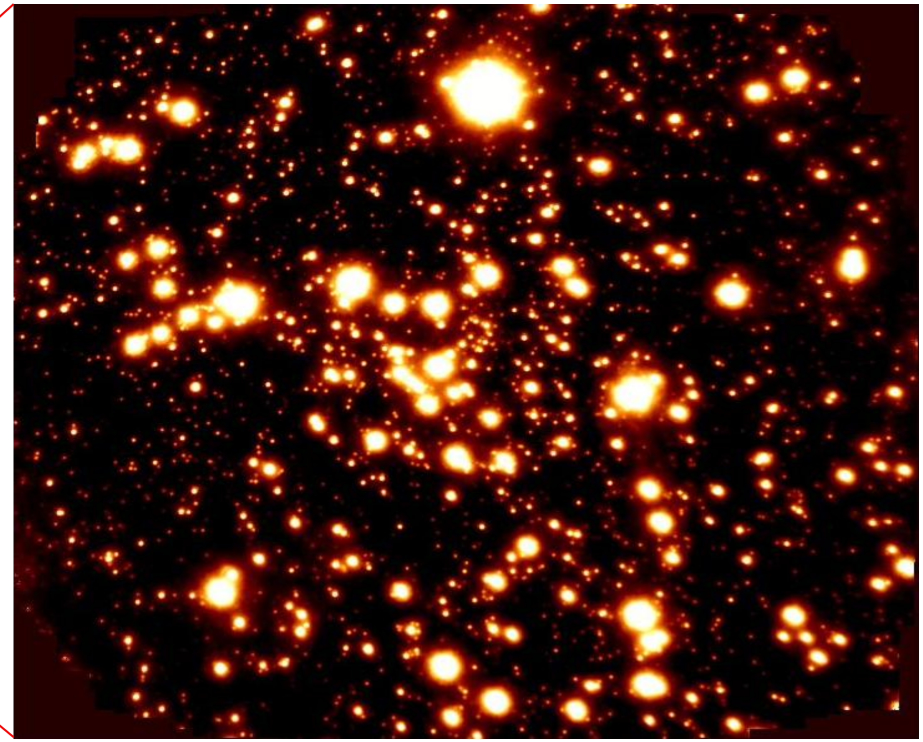

0.5 pc

(Becklin & Naugebauer 1968)

NACO AO NIR
Observations at the VLT in Chile
ince 1999
(+7 years NTT)

The MPE SHARP-Camera at the ESO New Technology Telescope (NTT) 1991-2002

Proper Motions from NTT Speckle Interferometry

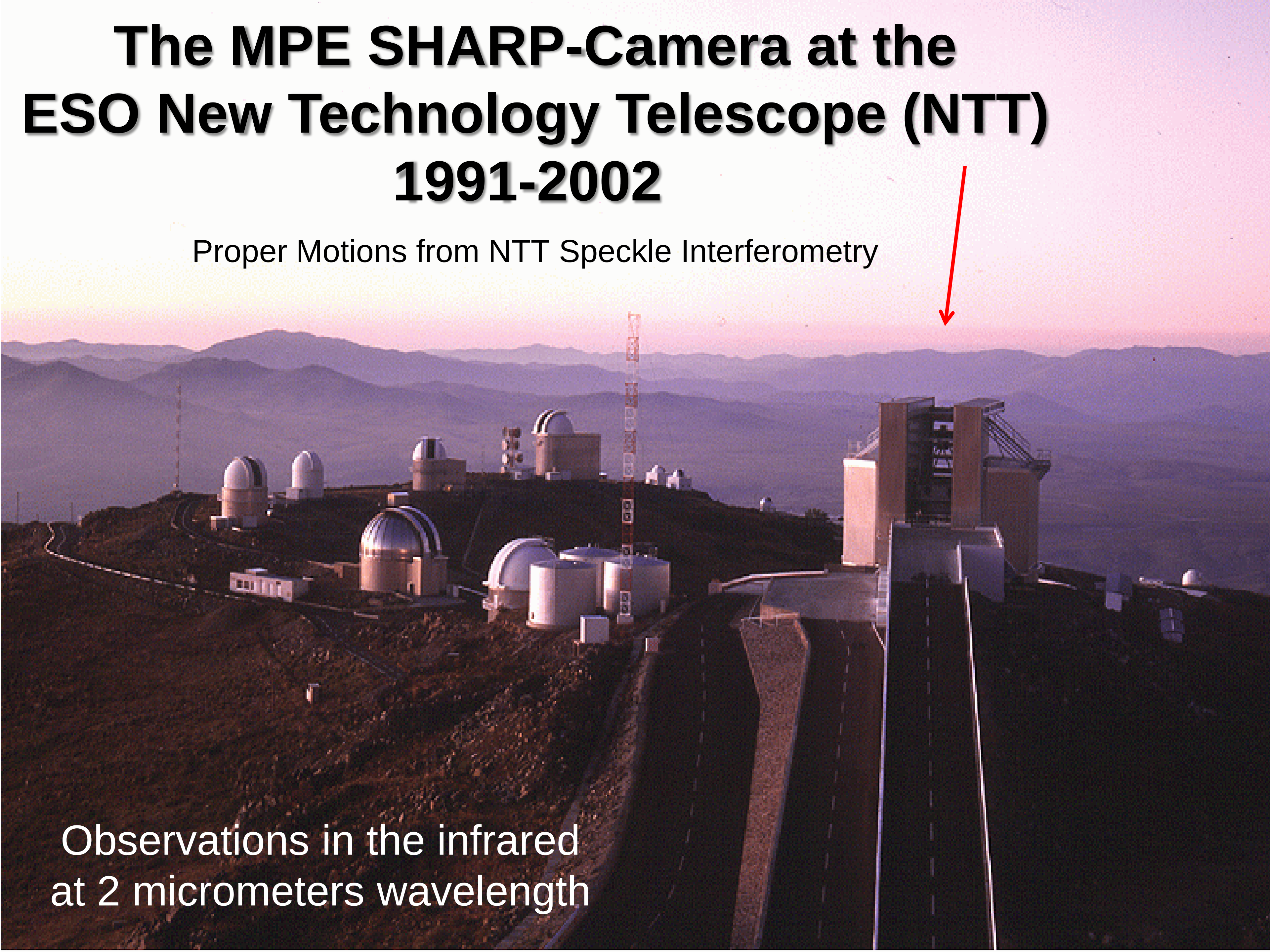

Observations in the infrared
at 2 micrometers wavelength

Speckle interferometry: via short term recordings (a few 100 ms) the disturbing influence of the atmosphere are frozen in and recorded.

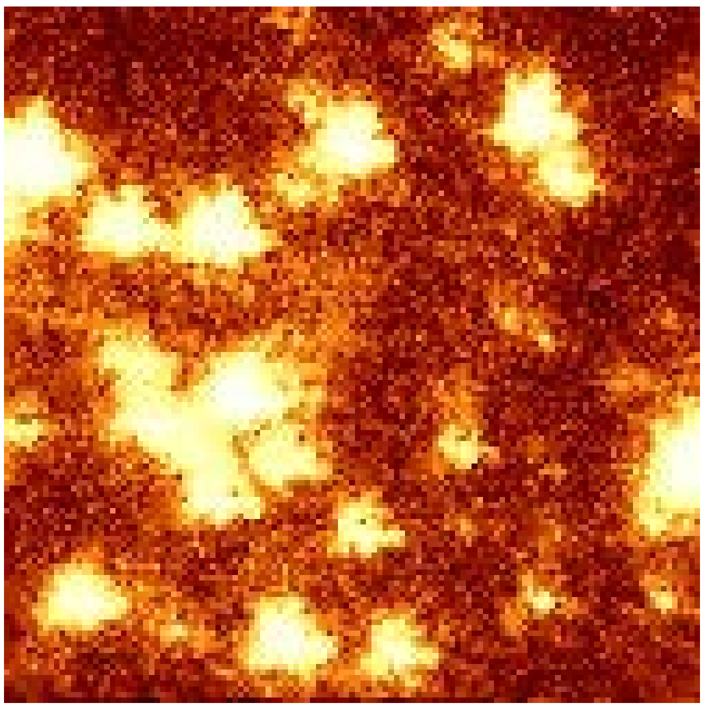

Short-term recordings from the SHARP Camera; Readout time 0.5 seconds

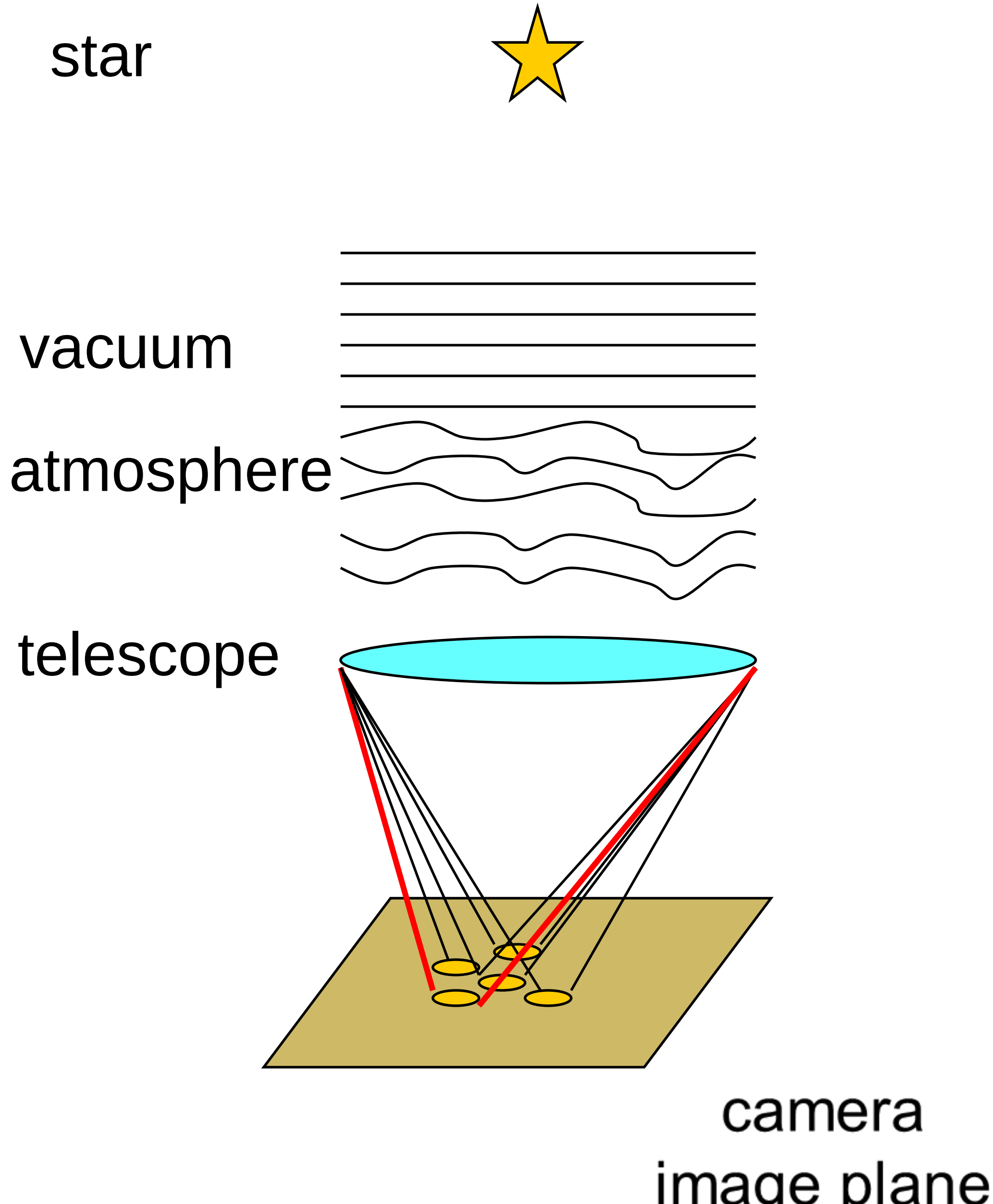

Proper motions

Stellar proper motions in the central 0.1 PC of the Galaxy
Eckart, A.; Genzel, R. 1996, Natue 383, 415

First Conclusive Evidence for a Massive Black Hole in the Center of the Milky Way
Eckart, Andreas; Genzel, Reinhard, 1997, MNRAS 284, 576

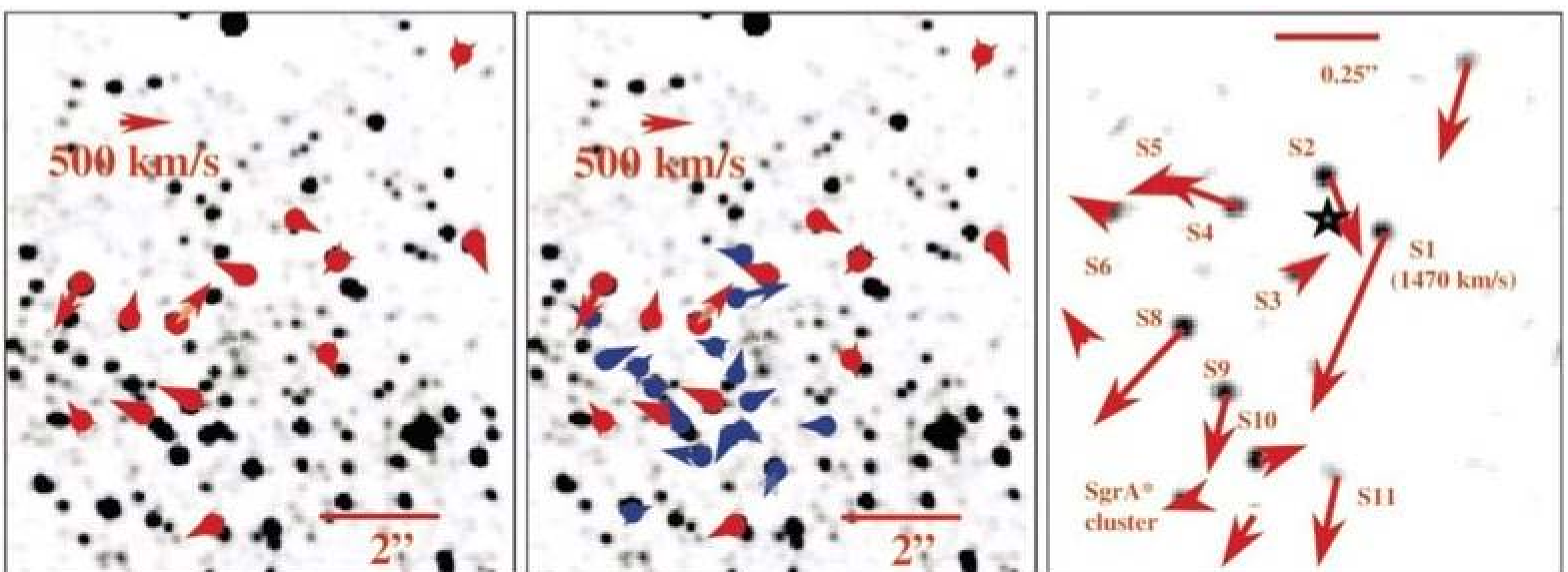

Proper motions

in the central SgrA* cluster 1992-2000

Eckart & Genzel, **1996**, Nature 383, 415;

Eckart & Genzel, **1997**, MNRAS 284, 576.

Ghez et al. **1998**, ApJ 509, 678.

0.5 "
$6x10^{16}$ cm
4000 AU

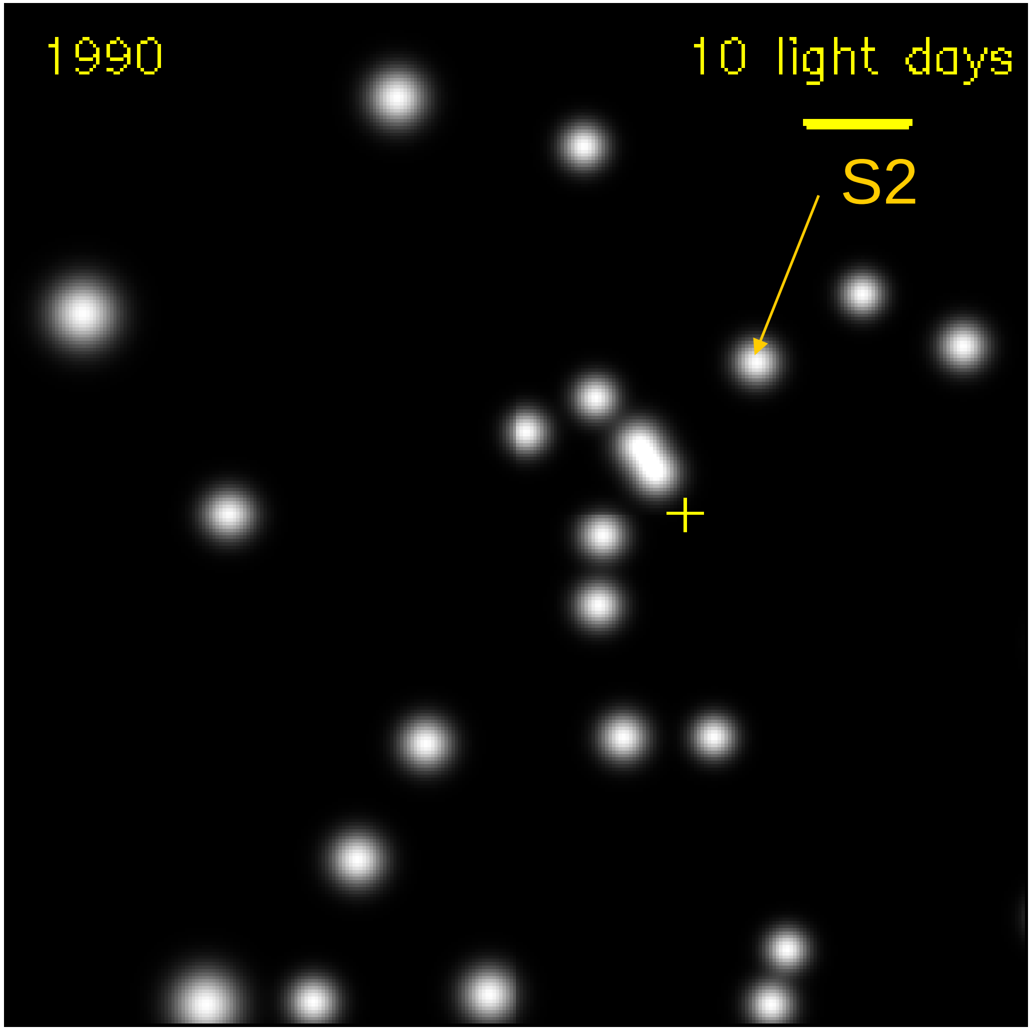

Very Large Telescope (VLT) – Chile - Paranal

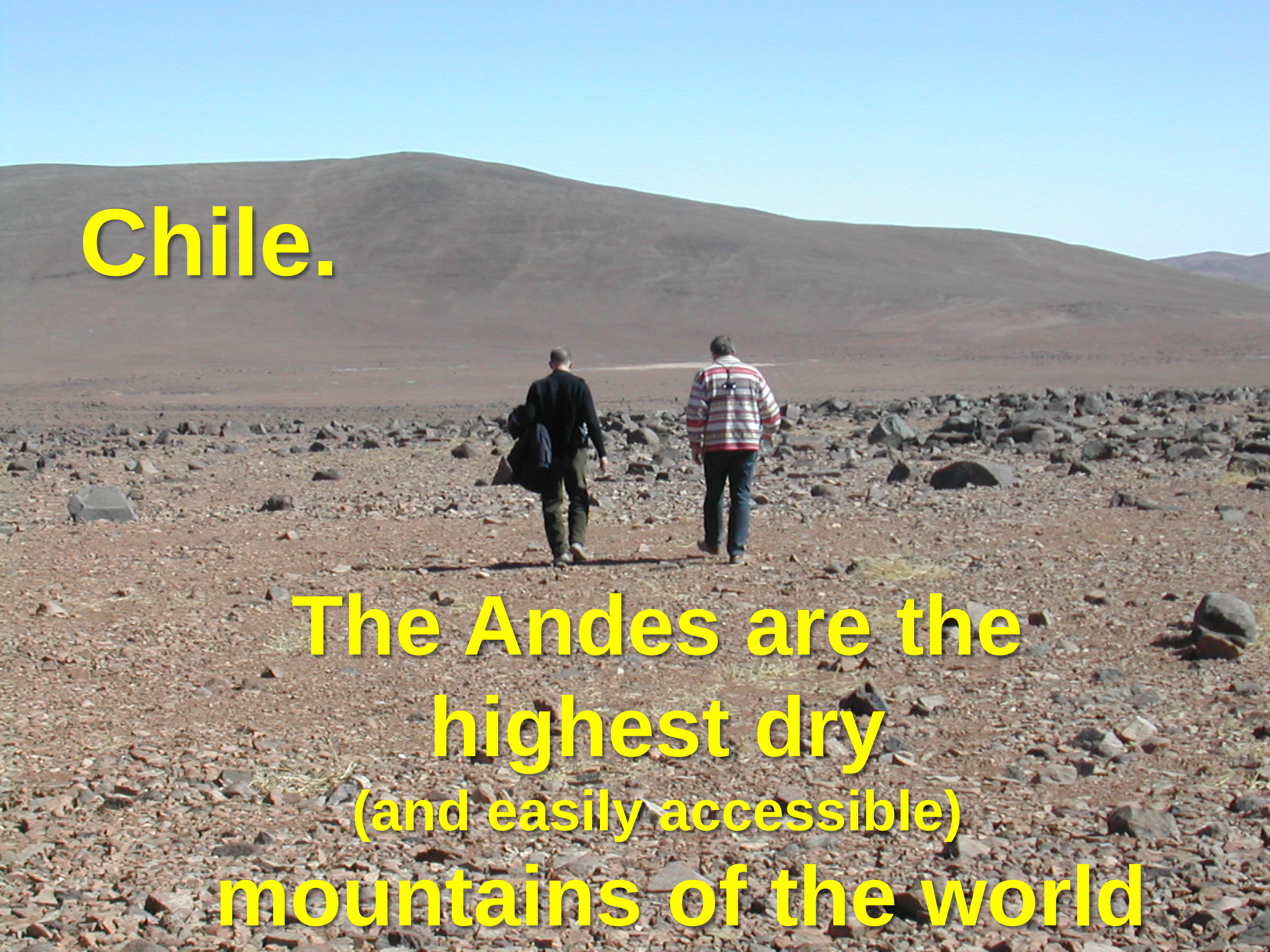
Chile.
The Andes are the
highest dry
(and easily accessible)
mountains of the world

Very Large Telescope (VLT) - Chile - Paranal

Proper Motions and Spectroscopy; Adaptive Optics at the VLT UT4

Observations in the infrared
at 2 micrometers wavelength


Telescopes
Garden with a fire pond that provides moisture.
Hier wohnen die Astronomen

Data Analysis

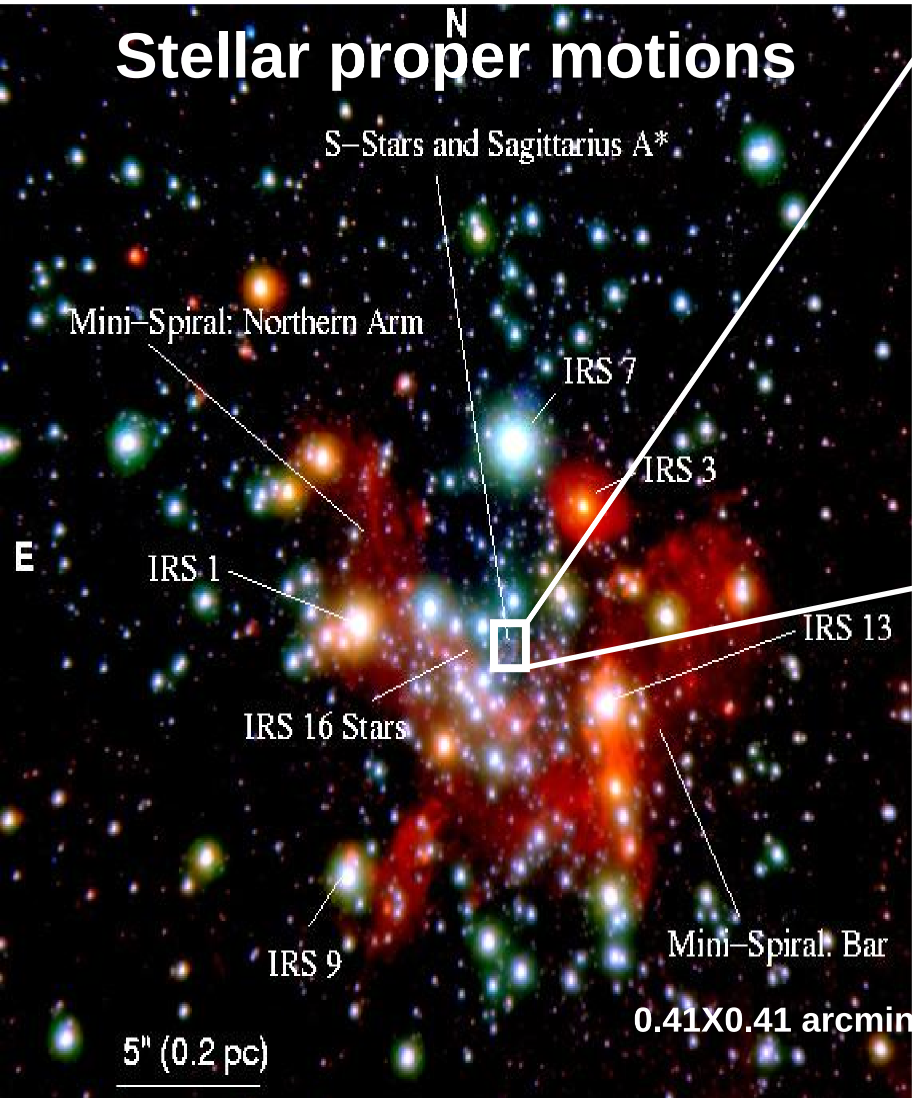

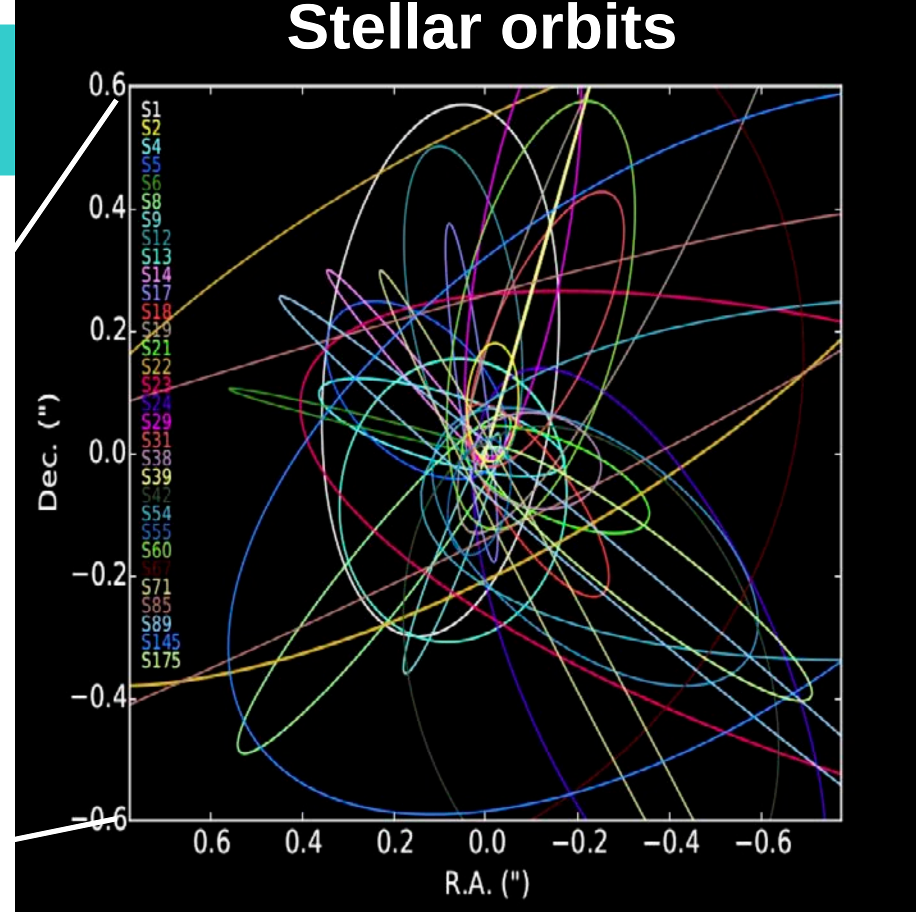

Orbits of almost 60 stars:

- **Ali et al. (2020)**
- **Parsa et al. (2018)**
- **Gillessen et al. (2017)**

First proper motions

- **Eckart & Genzel (1996/1997)**

Central Mass: 4 Million solar masses
Distance: 8 kpc ~ 27.000 light years

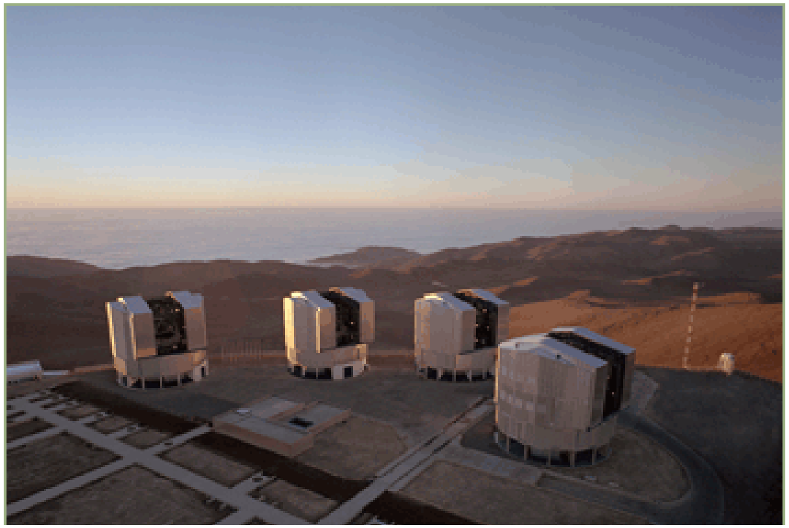

VLTI: GRAVITY

Principle Investigator: **Frank Eisenhauer (MPE, Garching)**

Builders: The Gravity consortium:

- Max-Planck-Institut für Exterterrestrische Physik (Garching),
- LESIA, Observatoire de Paris, Section de Meudon,
- Laboratoire d'Astrophysique, Observatoire de Grenoble,
- Max-Planck-Institut für Astronomie (Heidelberg),
- I. Physikalisches Institut, Universität zu Köln,
- SIM, Faculdade de Ciências da Universidade de Lisboa

Assistance via the European Southern Observatory

Difference between radio- and optical/infrared interferometry:

In the radio the signal transport and delay compensation is done via at intermediate frequencies via cable, tape and electronically. **In the optical/IR** you cannot stably and loss free mix down to an intermediate frequency, hence, it is done at sky frequecies via light and mirrors.

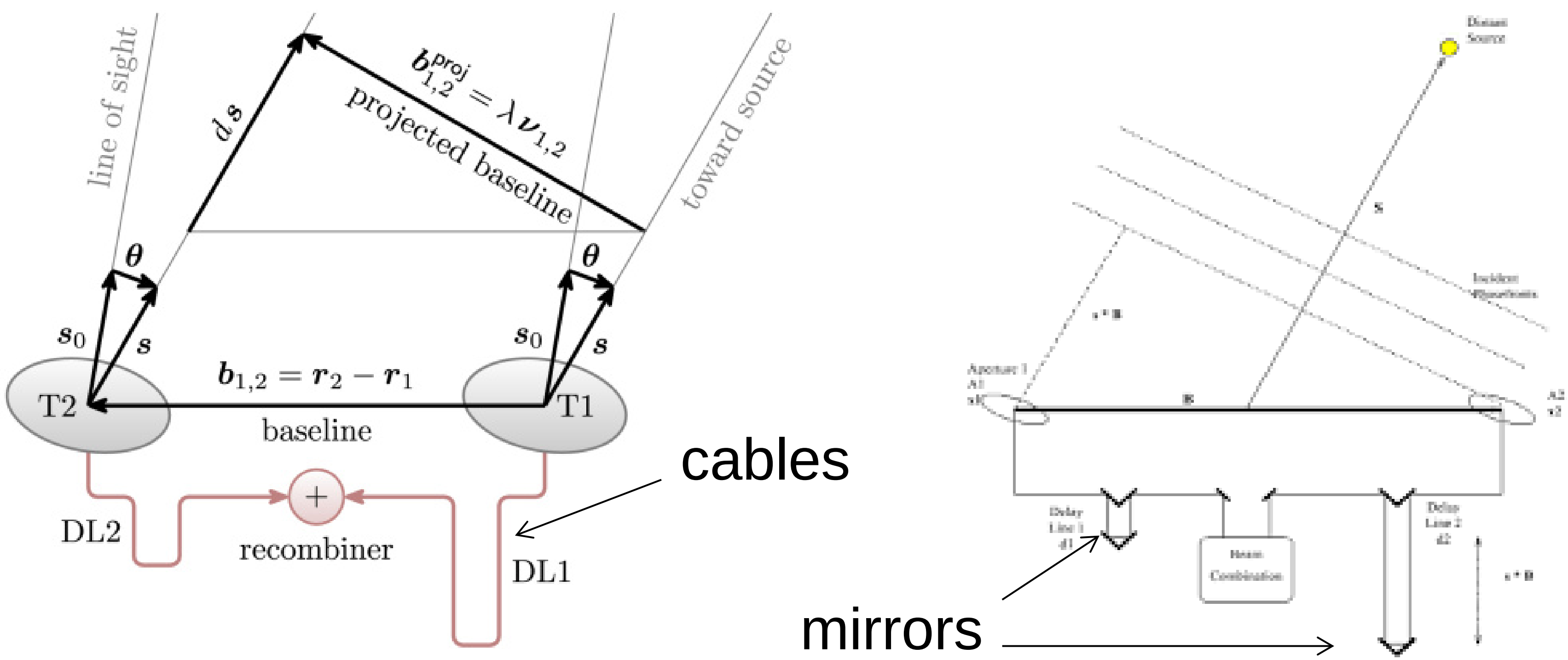

VLTI: VLT Interferometry with GRAVITY

High angular resolution measurements via connecting individual telescope

VLTI: VLT Interferometry with GRAVITY

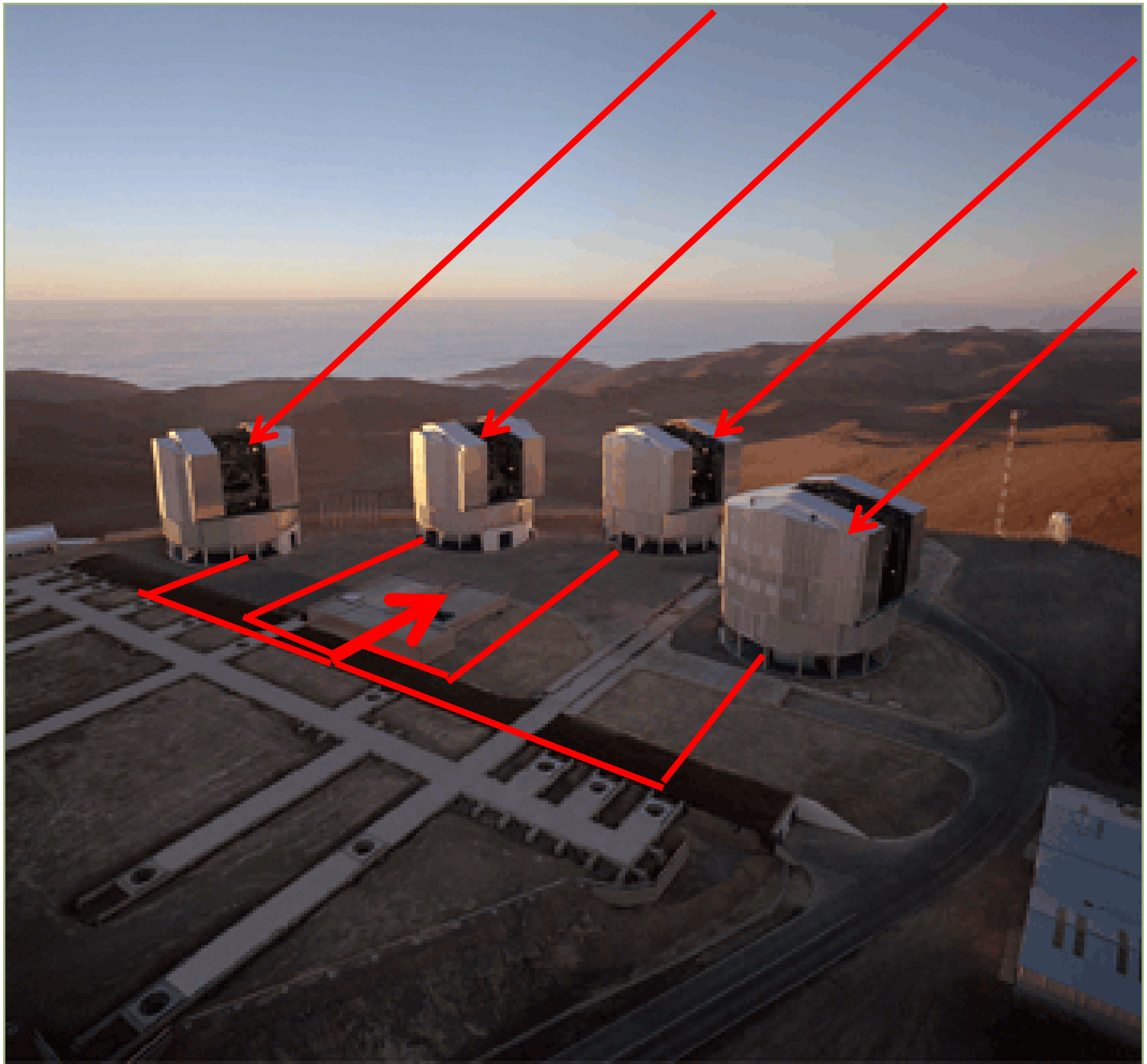

High angular resolution measurements via connecting individual telescope

VLTI: VLT Interferometry with GRAVITY

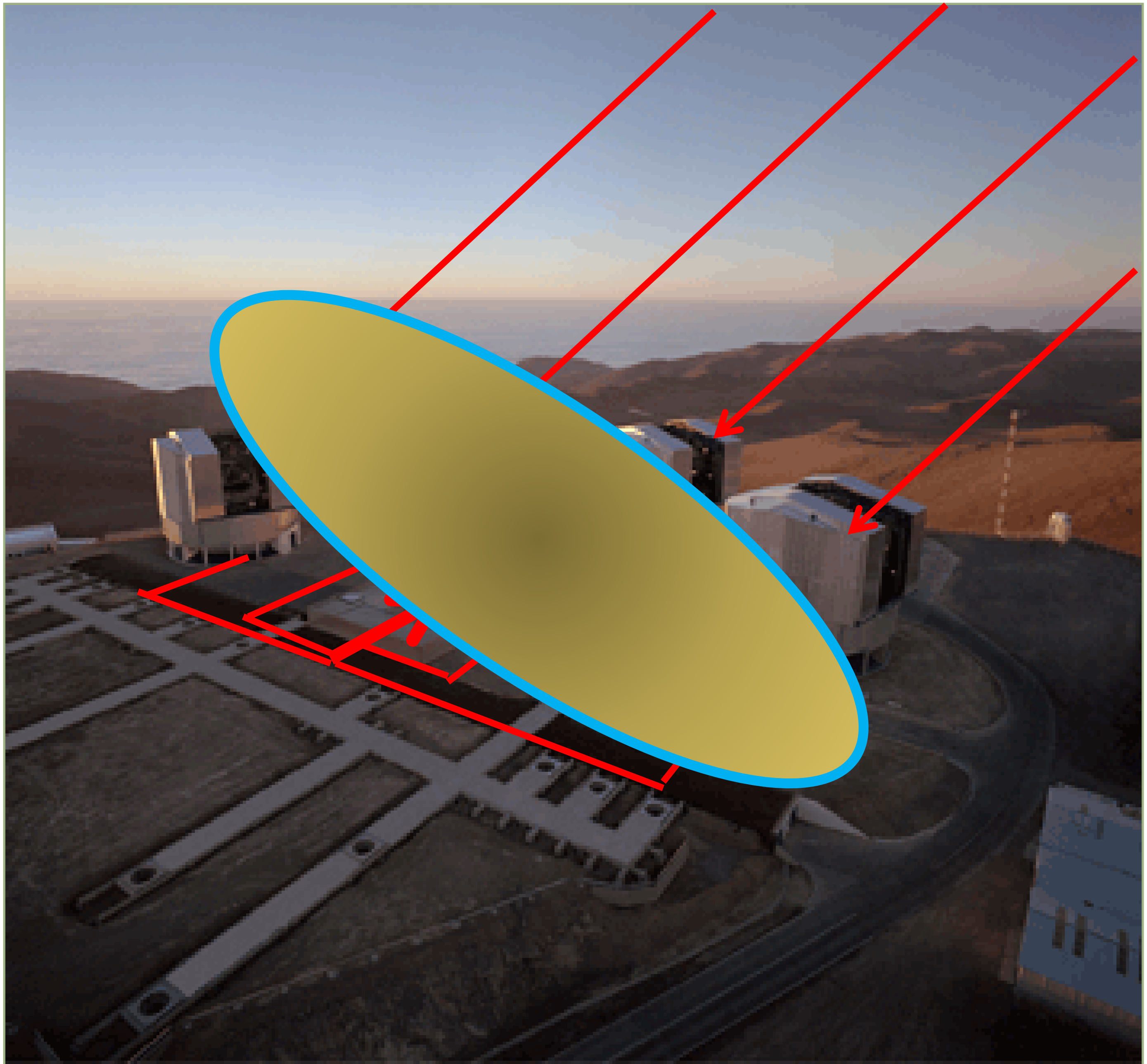

High angular resolution measurements via connecting individual telescope

This is how a telescope of much larger diameter is simulated

VLTI: VLT Interferometry with GRAVITY

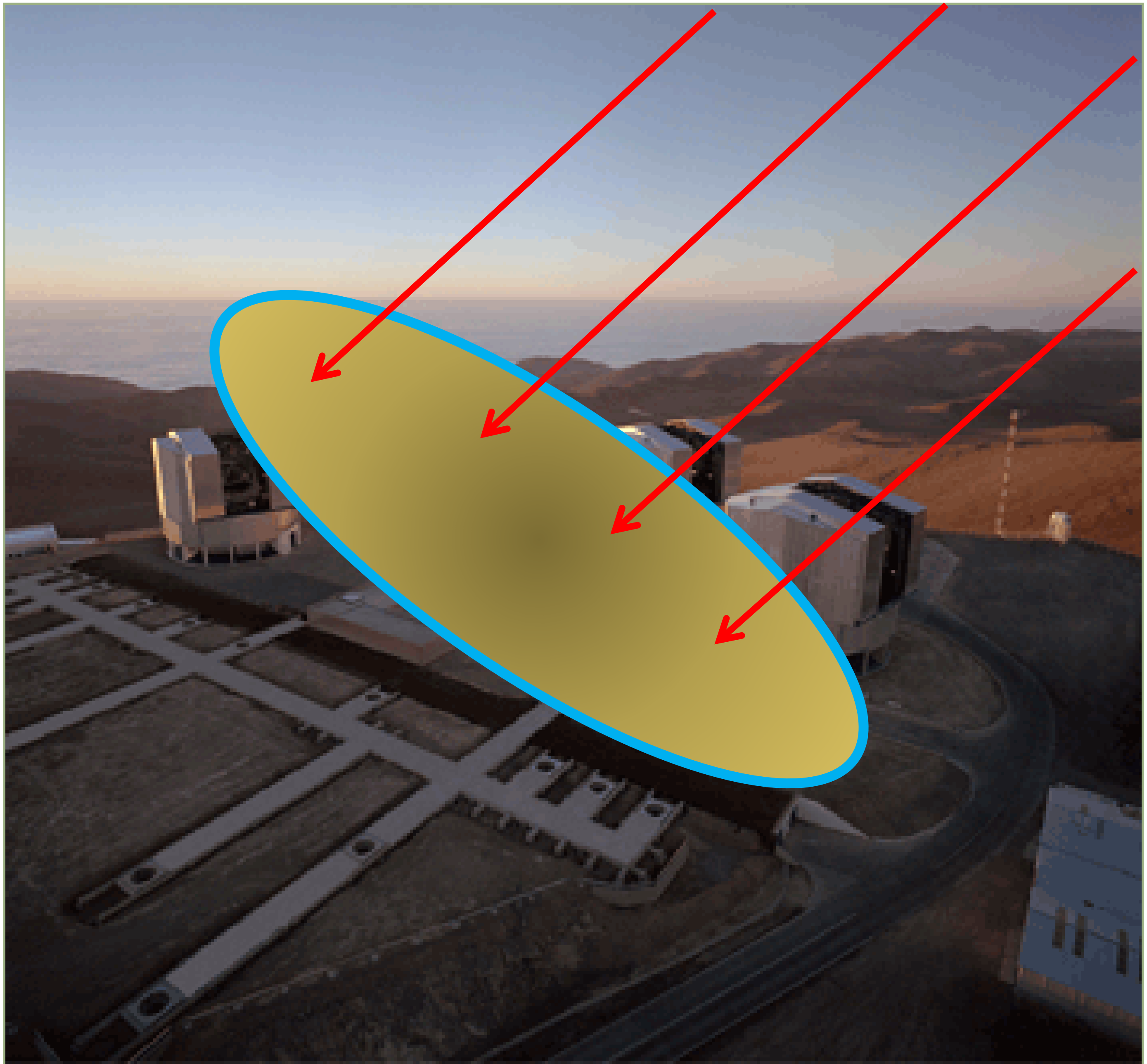

High angular resolution measurements via connecting individual telescope

This is how a telescope of much larger diameter is simulated

VLTI: GRAVITY

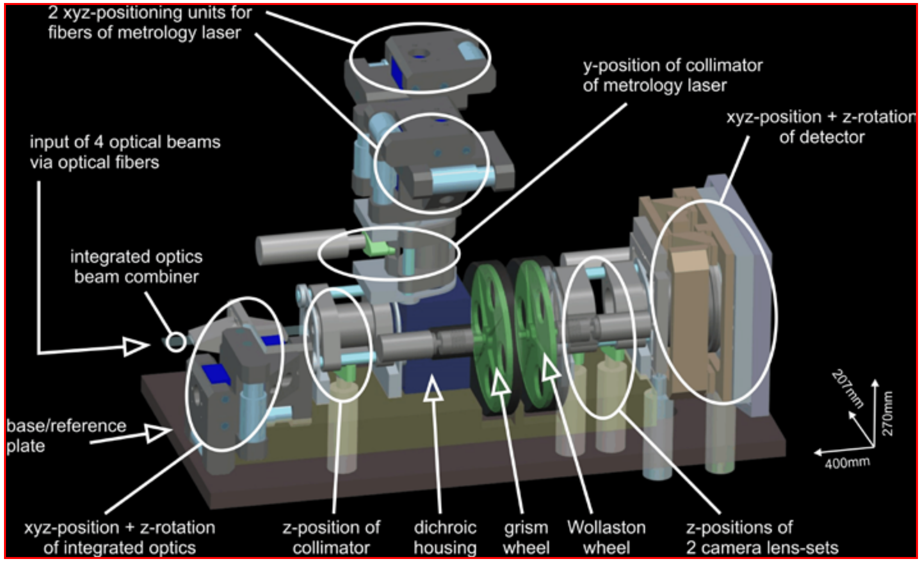

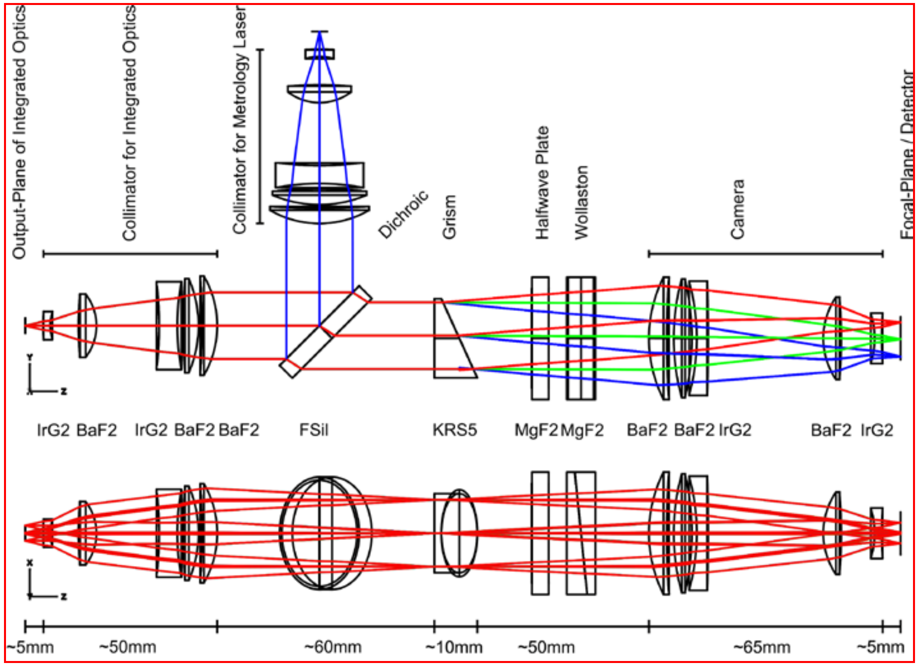

Cologne University provided the two beam combining spectrometers

Straubmeier, Eckart

METIS is <u>the</u> E-ELT instrument for $\lambda > 2.5\mu m$

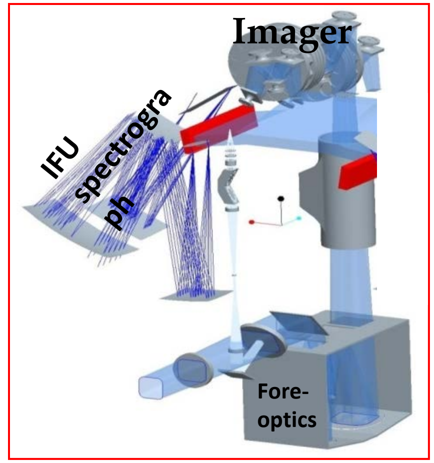

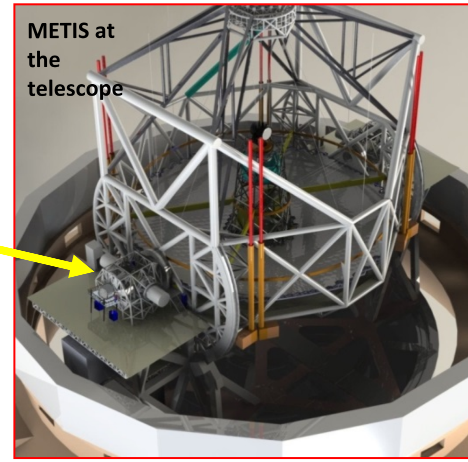

METIS Baseline:

- Diffraction limited **imager** [18″×18″] at L/M, N
    - incl. coronagraphy (N-band only)
    - incl. low-resolution (R ≤ 5000) long-slit
    - (incl. polarimeter (N-band))
- High resolution [R ~ 100,000]

IFU spectrograph [≥ 0.4″×1.6″] for L/M [2.9 – 5.3µm] band

PI: Bernhard Brandl

Der James-Webb-Satellit

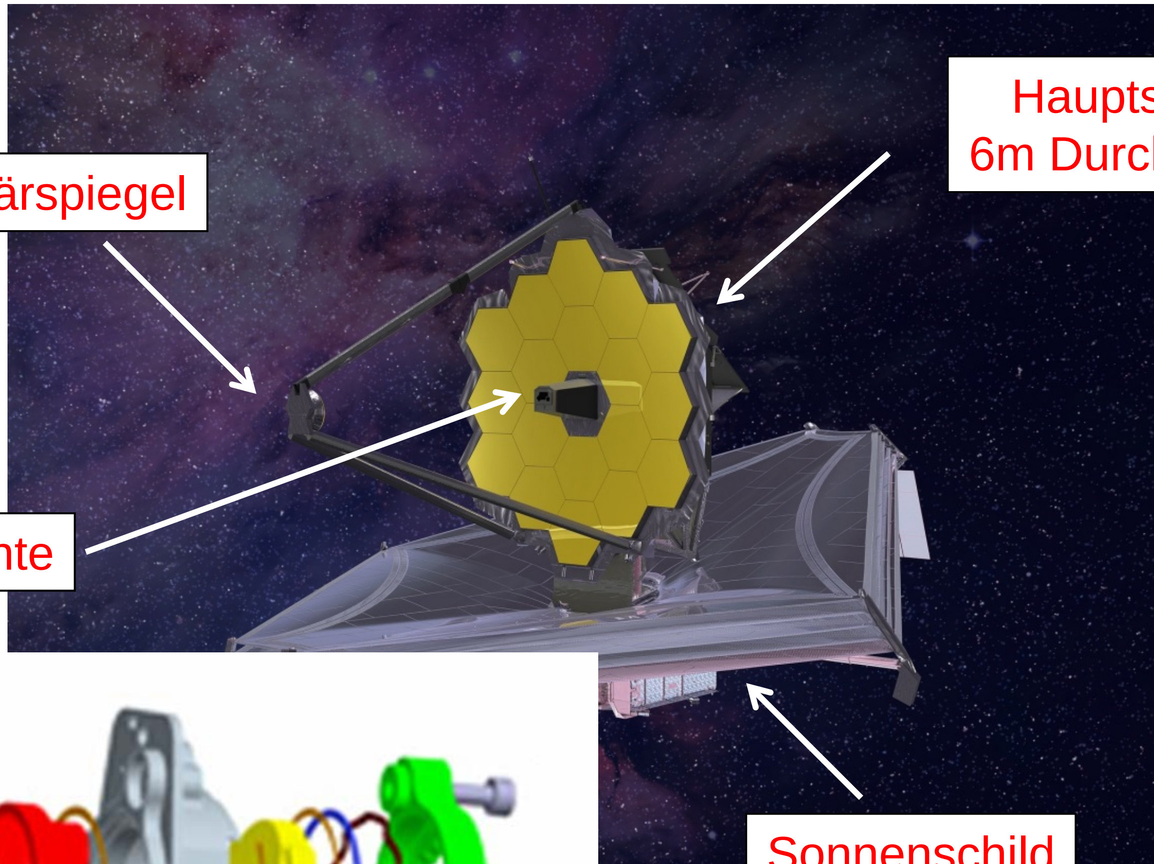

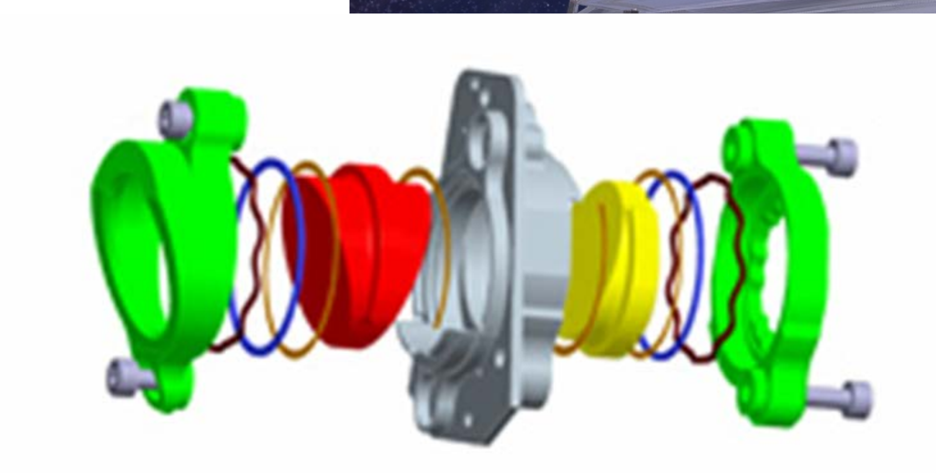

Detection of a Dust Component along the Line of Sight towards SgrA*

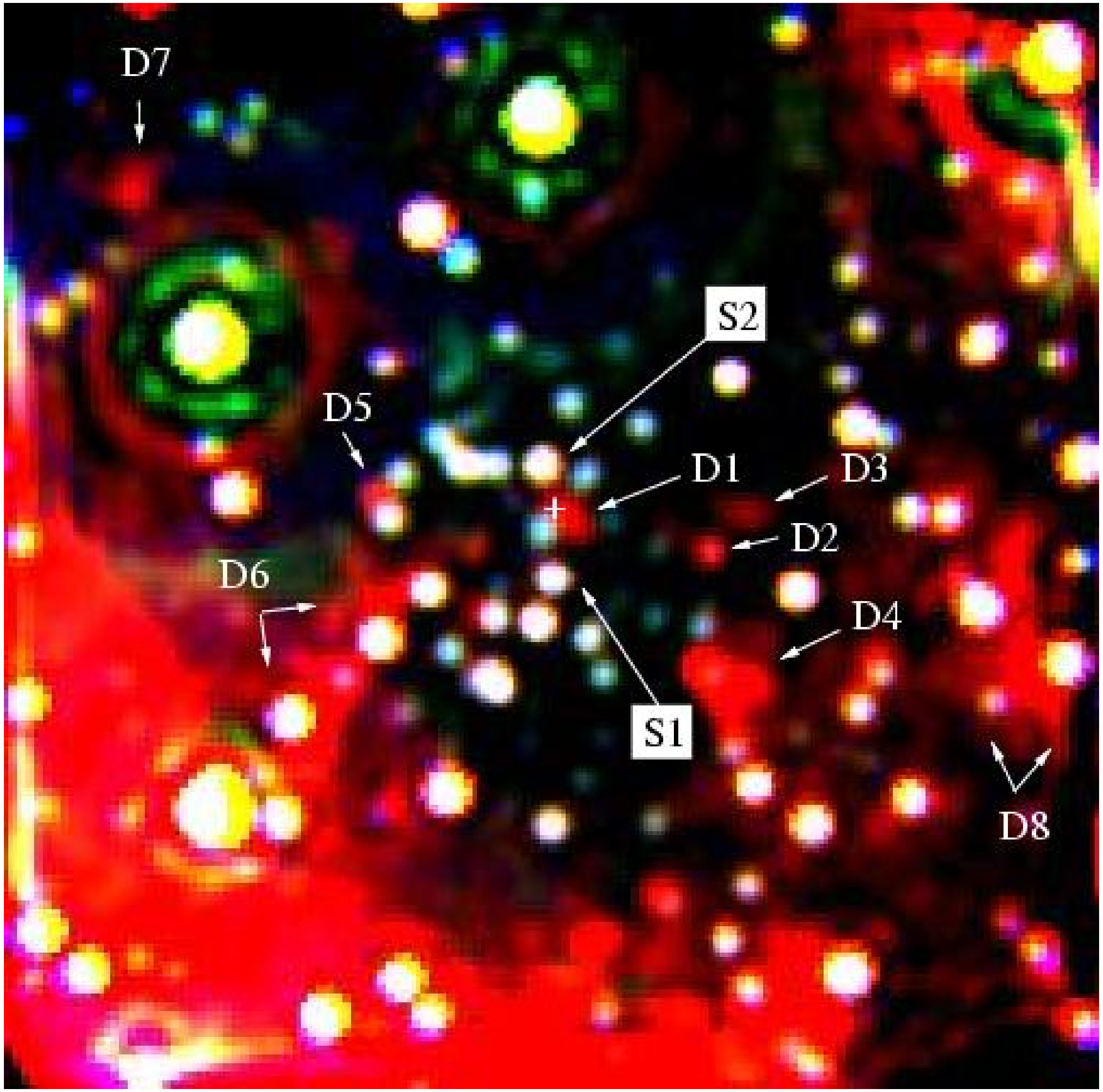

HKL multi-color image of the central 5“x5“ taken with NACO. L-band is in red.

Fore-/Backgrond dust component 26mas west of SgrA*
~1000 AU at 8 kpc

High angular resolution required in the MIR!!

Several of those dust blobs are seen across the field

Eckart et al. 2005

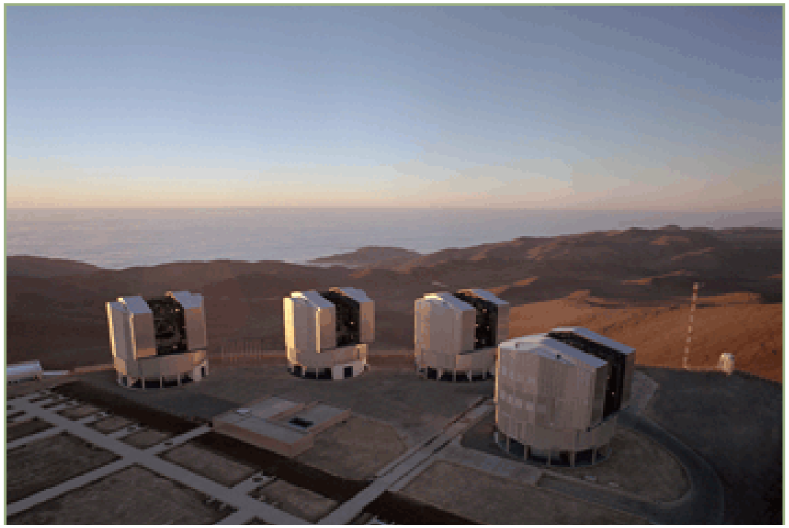

VLTI: GRAVITY+

Principle Investigator: **Frank Eisenhauer (MPE, Garching)**

Builders: The Gravity consortium:

- Max-Planck-Institut für Exterterrestrische Physik (Garching),
- LESIA, Observatoire de Paris, Section de Meudon,
- Laboratoire d'Astrophysique, Observatoire de Grenoble,
- Max-Planck-Institut für Astronomie (Heidelberg),
- I. Physikalisches Institut, Universität zu Köln,
- SIM, Faculdade de Ciências da Universidade de Lisboa

Assistance via the European Southern Observatory

Radio

The Galactic Center

400 km/s

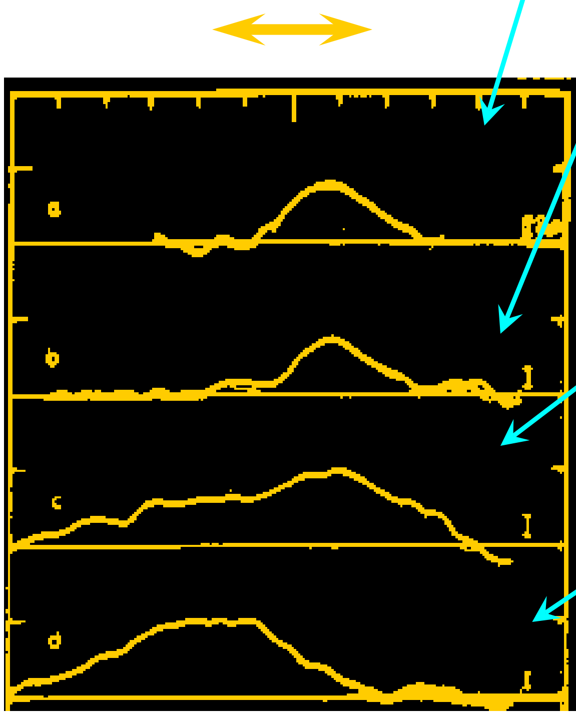

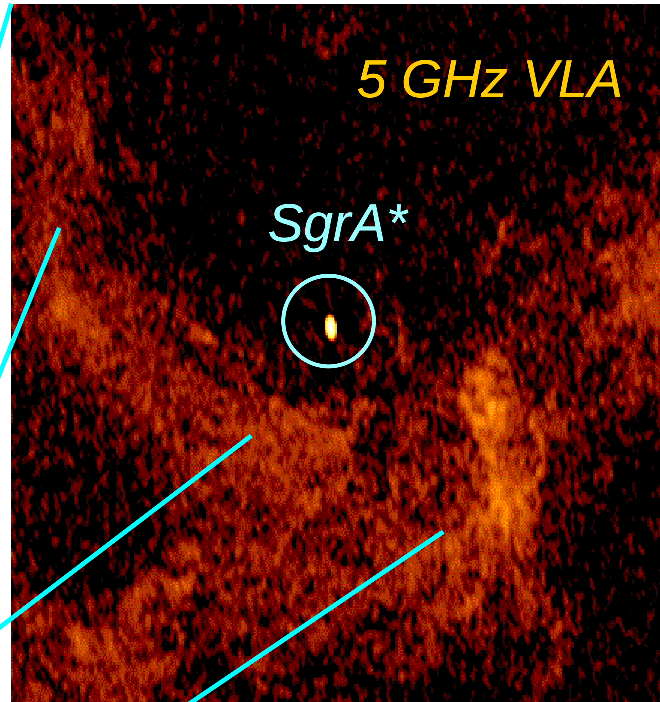

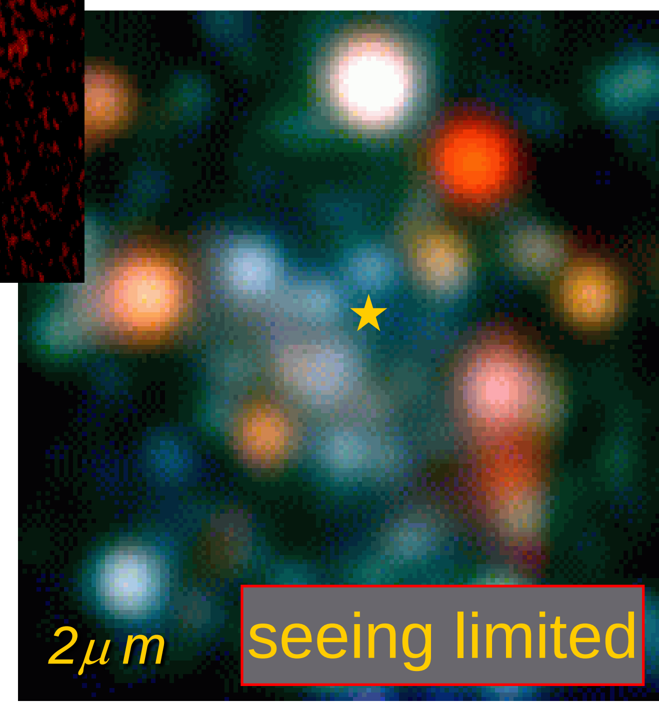

Wollman et al. 1977, Lacy et al. 1979, 1980,
Lo et al. 1983, DePoy and Sharp 1991

EVENT HORIZON TELESCOPE
mm-radio Very Long Baseline interferometry

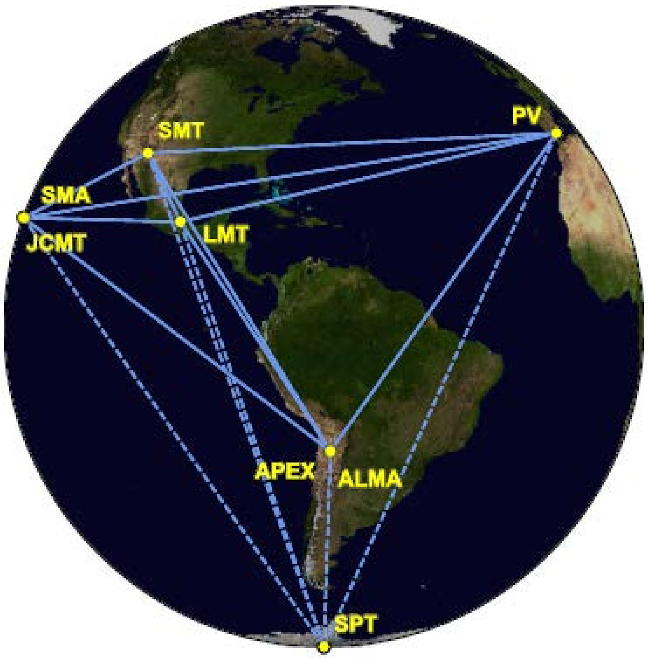

Figure 1. Eight stations of the EHT 2017 campaign over six geographic locations as viewed from the equatorial plane. Solid baselines represent mutual visibility on M87* (+12° declination). The dashed baselines were used for the calibration source 3C279 (see Papers III and IV).

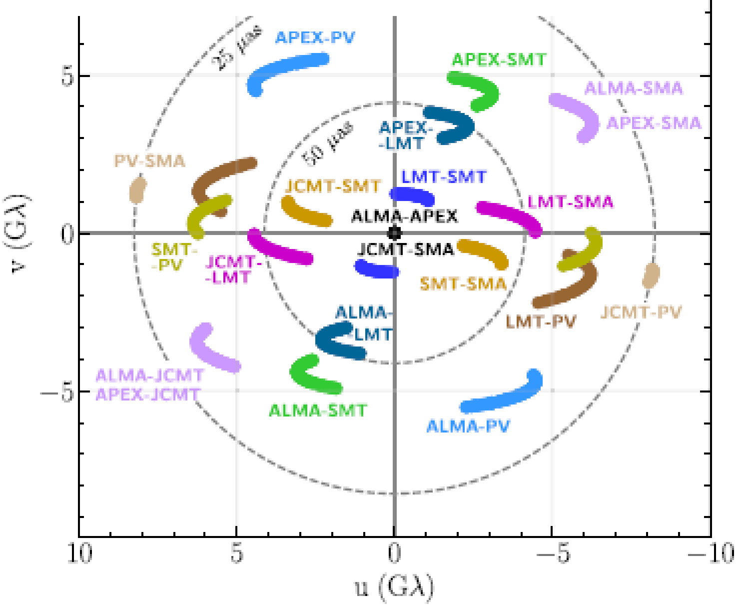

EVENT HORIZON TELESCOPE
mm-radio Very Long Baseline interferometry

First M87 Event Horizon Telescope Results. V. Physical Origin of the Asymmetric Ring

The Event Horizon Telescope Collaboration
(See the end matter for the full list of authors.)
Received 2019 March 4; revised 2019 March 12; accepted 2019 March 12; published 2019 April 10

First M87 Event Horizon Telescope Results. I. The Shadow of the Supermassive Black Hole

The Event Horizon Telescope Collaboration
(See the end matter for the full list of authors.)
Received 2019 March 1; revised 2019 March 12; accepted 2019 March 12; published 2019 April 10

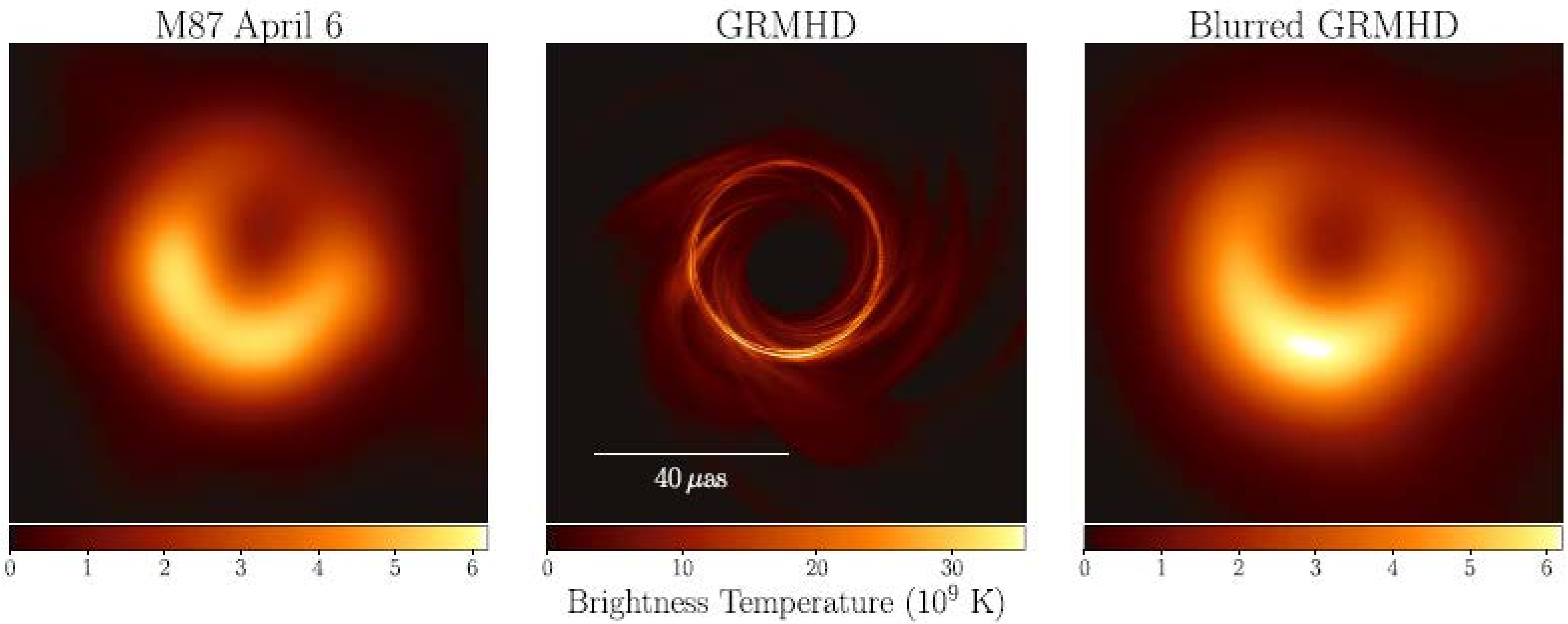

Figure 1. Left panel: an EHT2017 image of M87 from Paper IV of this series (see their Figure 15). Middle panel: a simulated image based on a GRMHD model. Right panel: the model image convolved with a 20 μas FWHM Gaussian beam. Although the most evident features of the model and data are similar, fine features in the model are not resolved by EHT.

EVENT HORIZON TELESCOPE
mm-radio Very Long Baseline interferometry

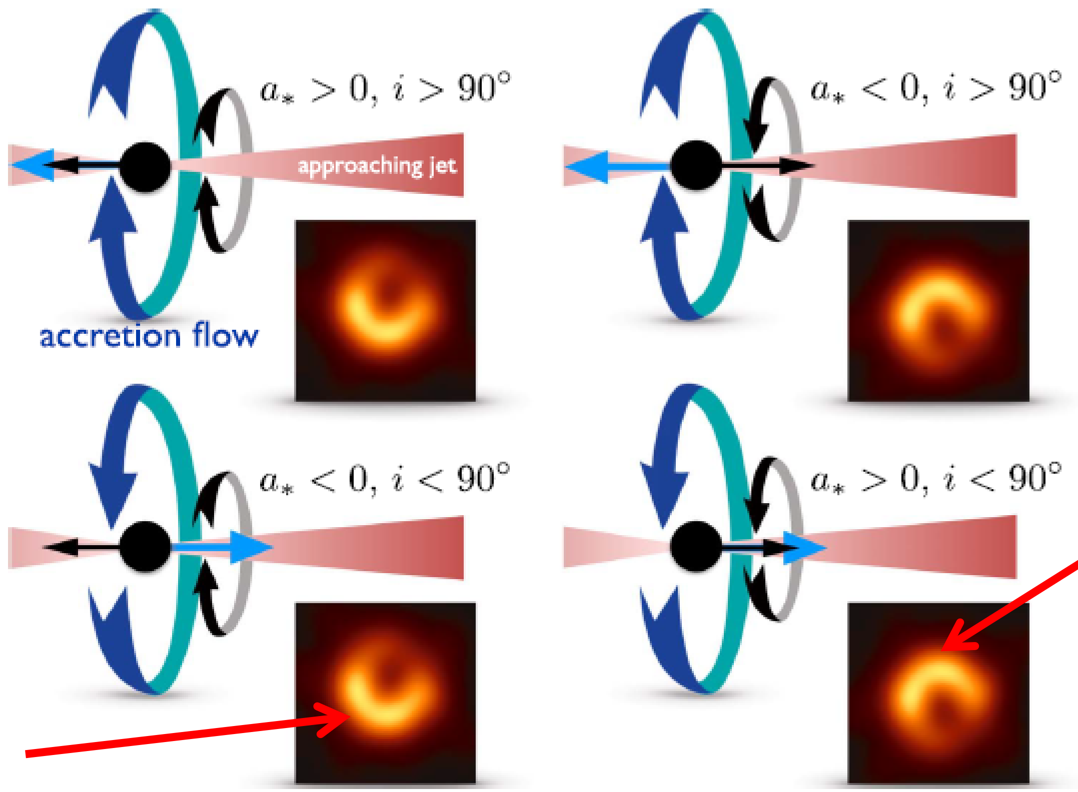

boosted side is brightended by aberration

boosted side is brightended by aberration

Figure 5. Illustration of the effect of black hole and disk angular momentum on ring asymmetry. The asymmetry is produced primarily by Doppler beaming: the bright region corresponds to the approaching side. In GRMHD models that fit the data comparatively well, the asymmetry arises in emission generated in the funnel wall. The sense of rotation of both the jet and funnel wall are controlled by the black hole spin. If the black hole spin axis is aligned with the large-scale jet, which points to the right, then the asymmetry implies that the black hole spin is pointing away from Earth (rotation of the black hole is clockwise as viewed from Earth). The blue ribbon arrow shows the sense of disk rotation, and the black ribbon arrow shows black hole spin. Inclination i is defined as the angle between the disk angular momentum vector and the line of sight.

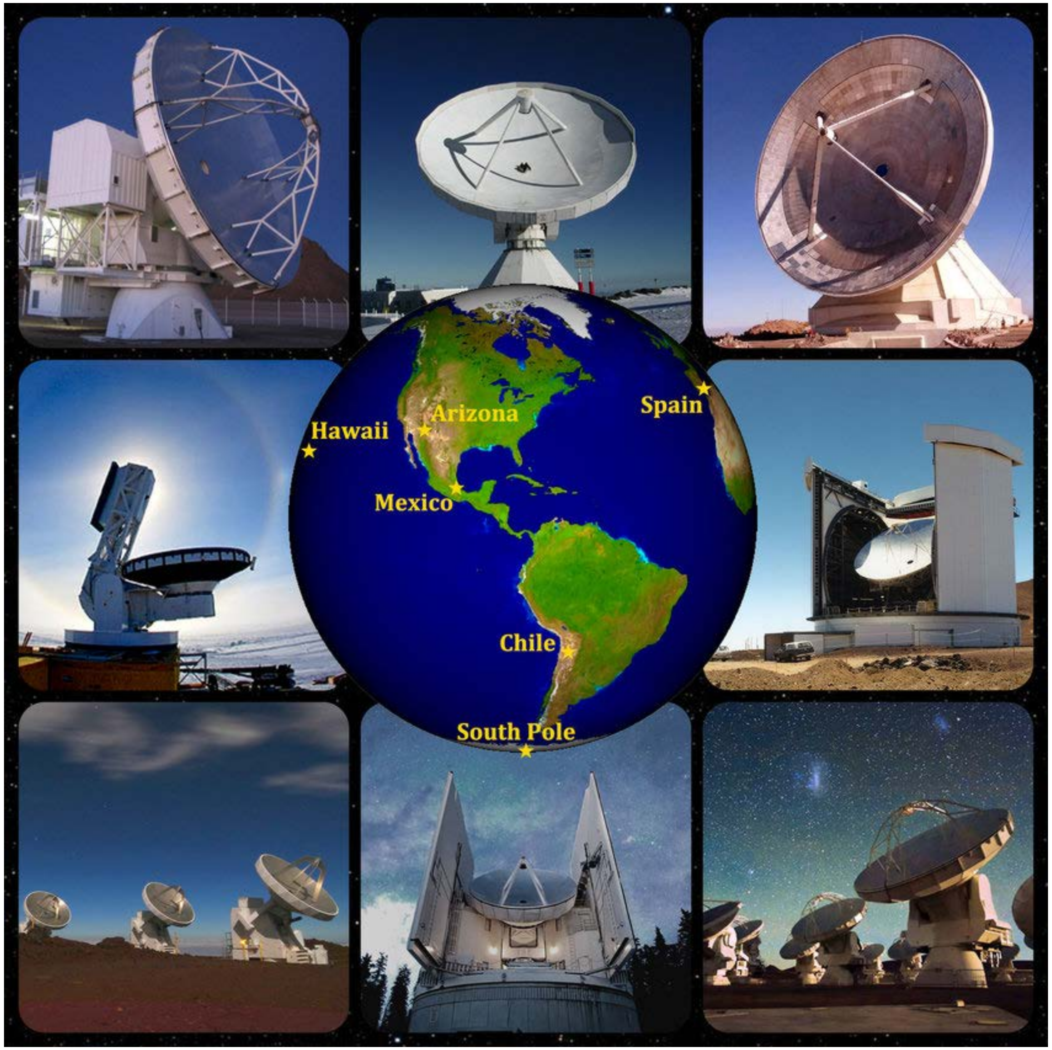

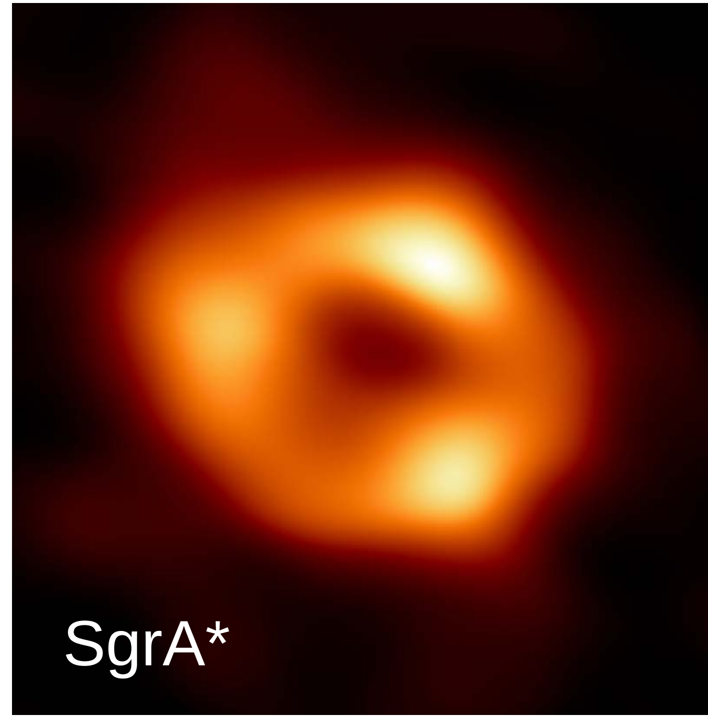

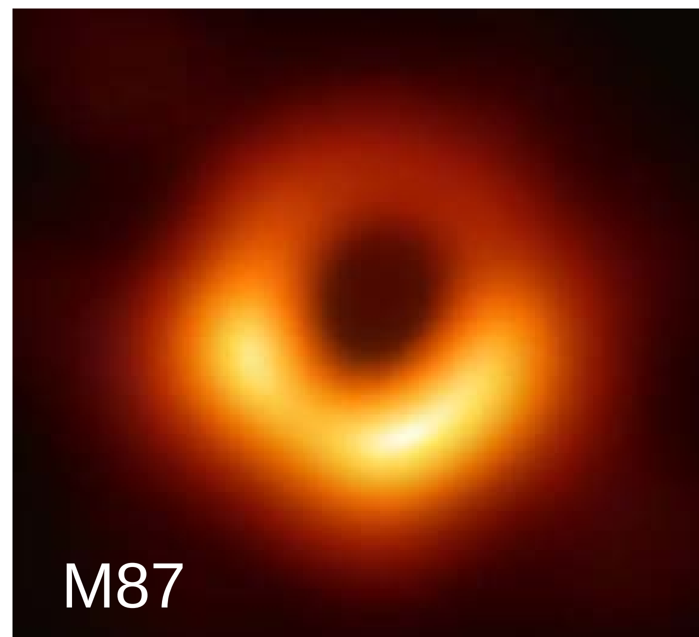

Event Horizon Telescope 2019/22

Breakthrough Prize in Fundamental Physics awarded to the Event Horizon Telescope Collaboration

Past and Future Cosmologically

Past and Future Instrumentally

- Past and Future Observationally

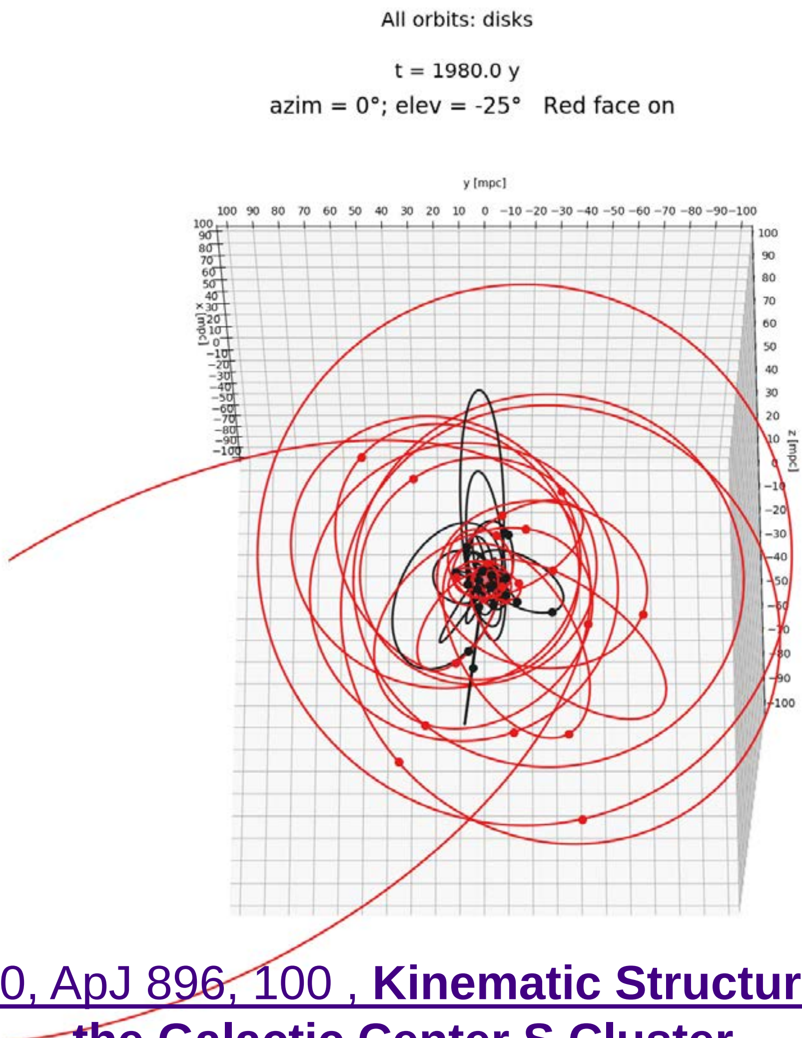

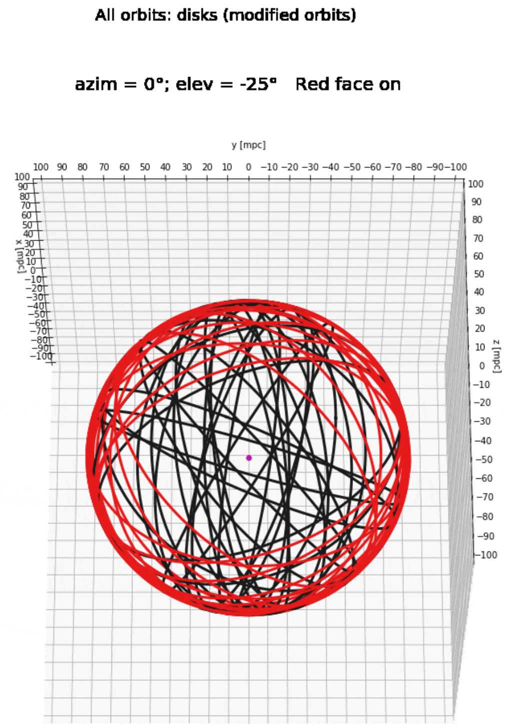

2020, ApJ 896, 100 , **Kinematic Structure of the Galactic Center S Cluster**

Ali, Basel; Paul, Daria; Eckart, Andreas; Parsa, Marzieh; Zajacek, Michal; Peißker, Florian; Subroweit, Matthias; Valencia-S., Monica; Thomkins, Lauritz; Witzel, Gunther

Kinematic structure of the S-cluster:
Two orthogonal thick disks
Ali et al. 2020

Visualization of Results

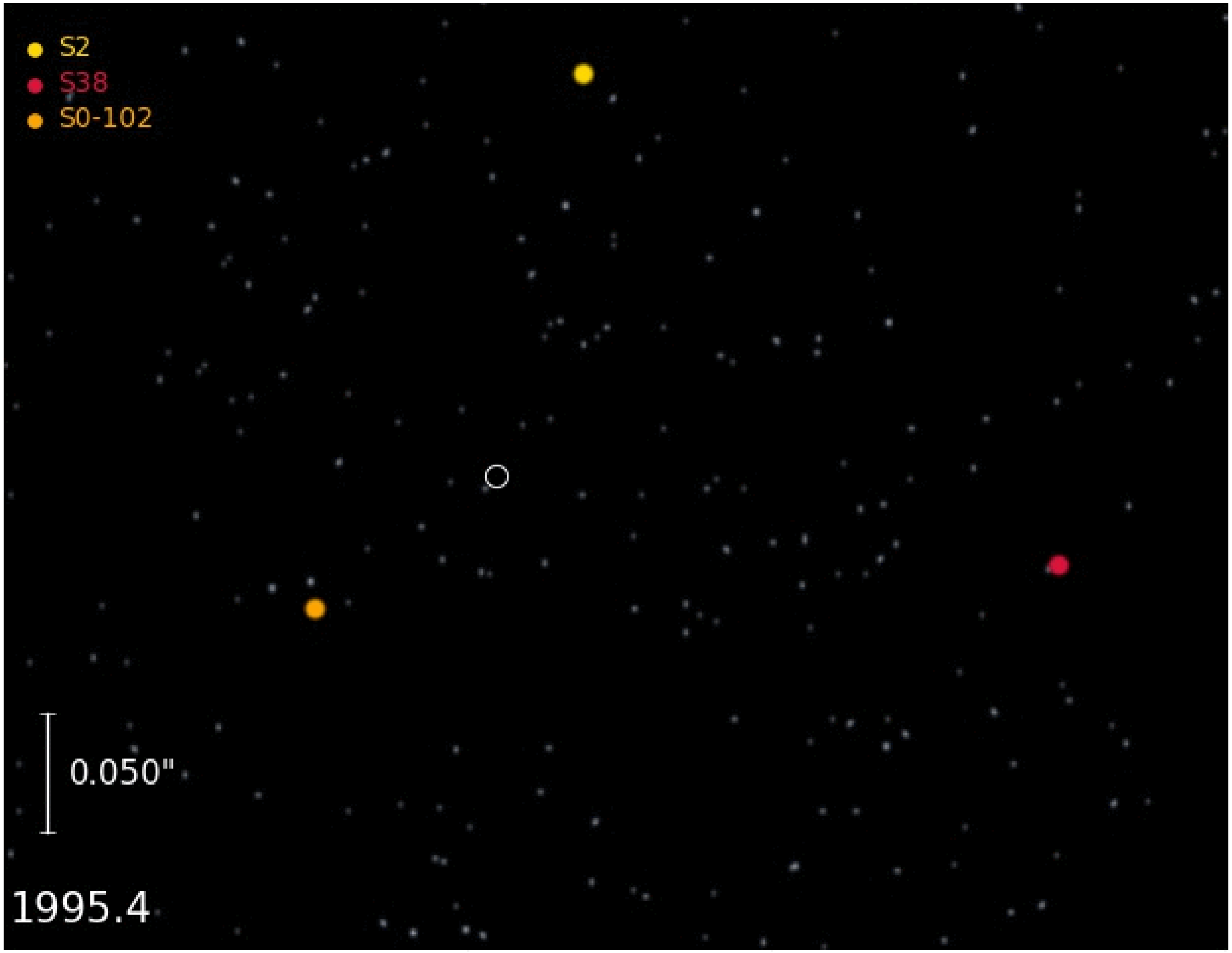

ESO press annoncement 9 August <u>2017</u>: ann17051:
Hint of Relativity Effects in Stars Orbiting the Supermassive Black Hole at Centre of Galaxy

Parsa et al. 2017

Results

- The best estimates for the mass and the distance to Sgr A* are:

$$M_{BH} = (4.15 \pm 0.13 \pm 0.57) \times 10^{6} M_{sun}$$

$$R_0 = 8.19 \pm 0.11 \pm 0.34 \ kpc$$

- The change in the argument of periapse of S2 is

$$\Delta\omega_{obs} = 14\,' \pm 3$$

$$\Delta\omega_{expected} = 11\,'$$

- The changes in the orbital elements of S2 imply relativistic parameter of:

$$Y_{obs} = 0.00088 \ \pm 000065$$

$$Y_{expected} = 0.00065$$

Eckart et al. 2018
Parsa et al. 2017

Relativistic Parameter Y:
Zucker et al. 2006

$$Y = \frac{r_s}{r_p}$$

Schwarzschild Precession

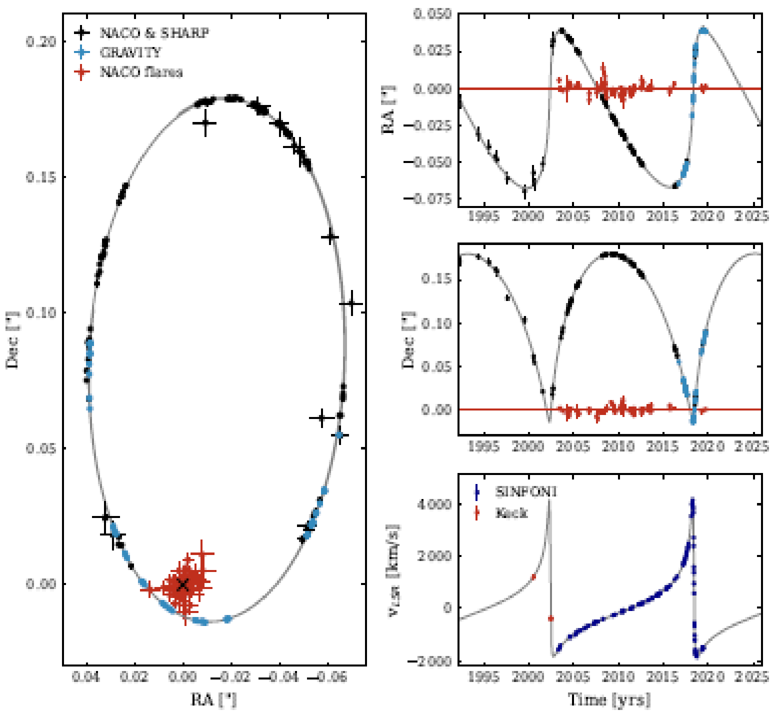

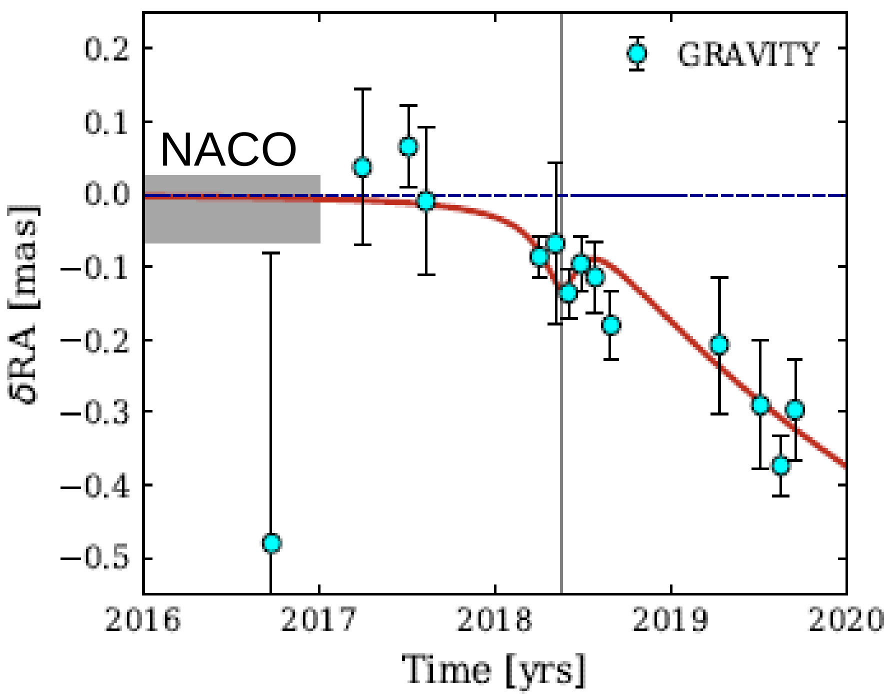

Detection of the Schwarzschild precession in the orbit of the star S2 near the Galactic centre massive black hole

Gravity Collaboration; 2020, A&A 636, L5

Gravitational Redshift

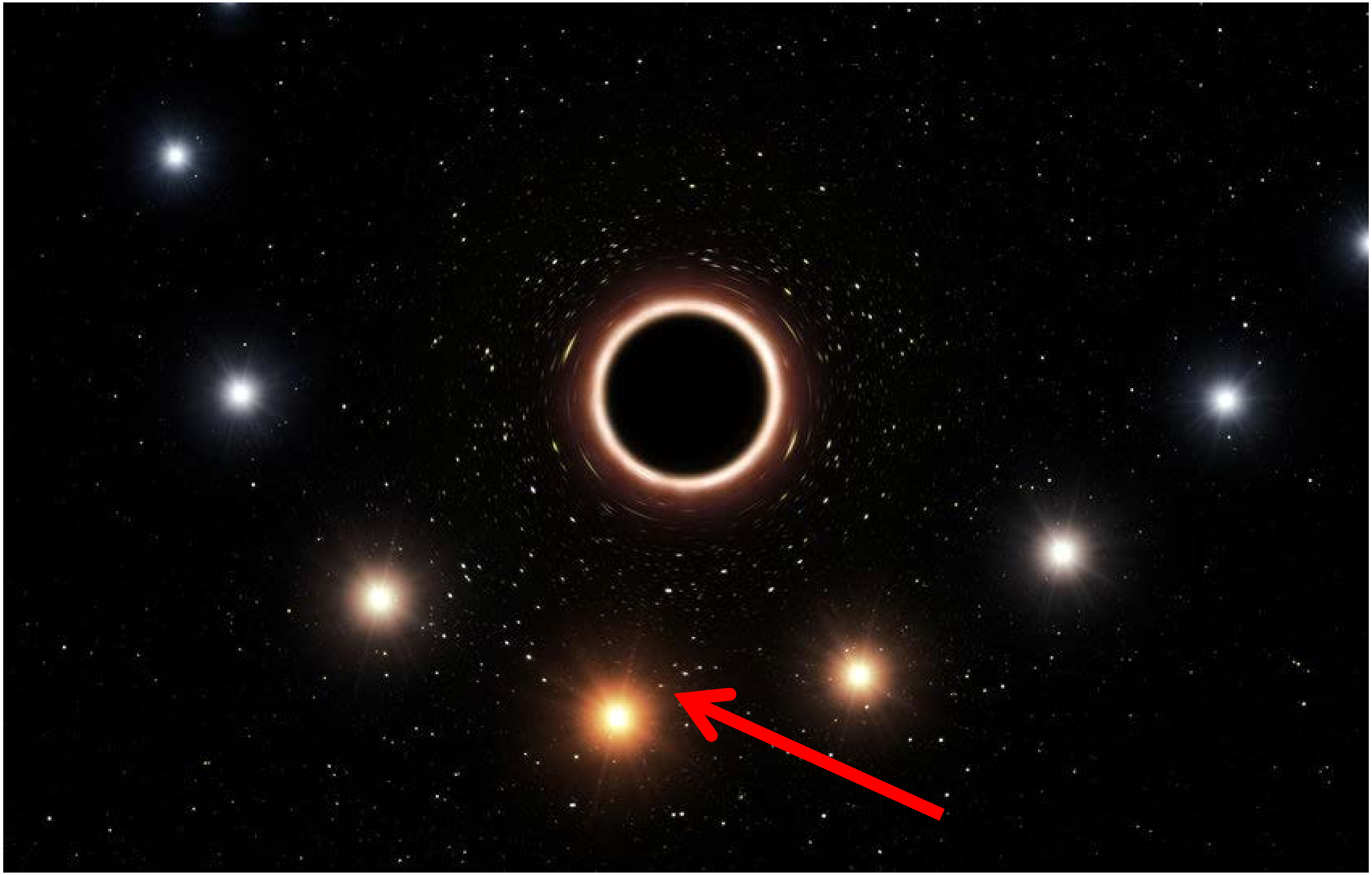

Observed redshift as a function of the 3 dimensional velocity β

$$z = \Delta\lambda / \lambda = B_0 + B_1\beta + B_2\beta^2 + O(\beta^3)$$

Relativistic Redshift

$$B_2 = B_{2,D} + B_{2,G} = \frac{1}{2} + \frac{1}{2}$$

$B_{2,G}$: gravitational redshift effect

$$z_G \equiv r_s / 4a + \frac{1}{2}\beta^2 = B_{0,G} + B_{2,G}\beta^2$$

$B_{2,D}$: special relativistic transverse Doppler effect

$$z_D \equiv (1 + \beta\cos\vartheta)(1 - \beta^2)^{-1/2} - 1$$

$$z_D \equiv z_{Newton} + z_{transverse} = \beta\cos\vartheta + \beta^2 / 2 = B_1\beta + B_{2,D}\beta^2$$

Zucker et al. 2006

$O(\beta^2) -$ effects should be observable with today's instrumentation:

$$(B_{2,D} + B_{2,G})\beta_P^2 \sim 10^{-3} > \frac{\delta\lambda}{\lambda} \sim 10^{-4}$$

$$\beta_P \sim \frac{v_{Peri}}{c}$$

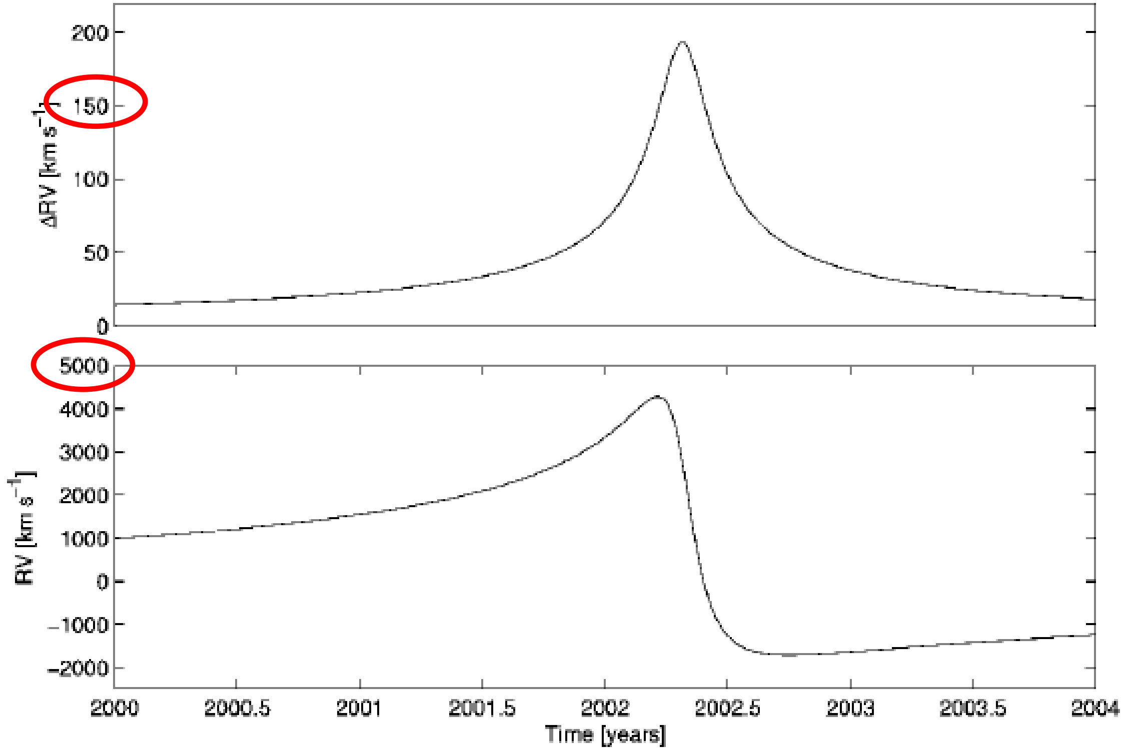

Contribution of the $O(\beta^2) -$ effects

full relativistic radial velocity of S2 near periaps

S2 e=0.88, r = 1500 rs

S14 e=0.94 r = 1400 rs

Zucker et al. 2006

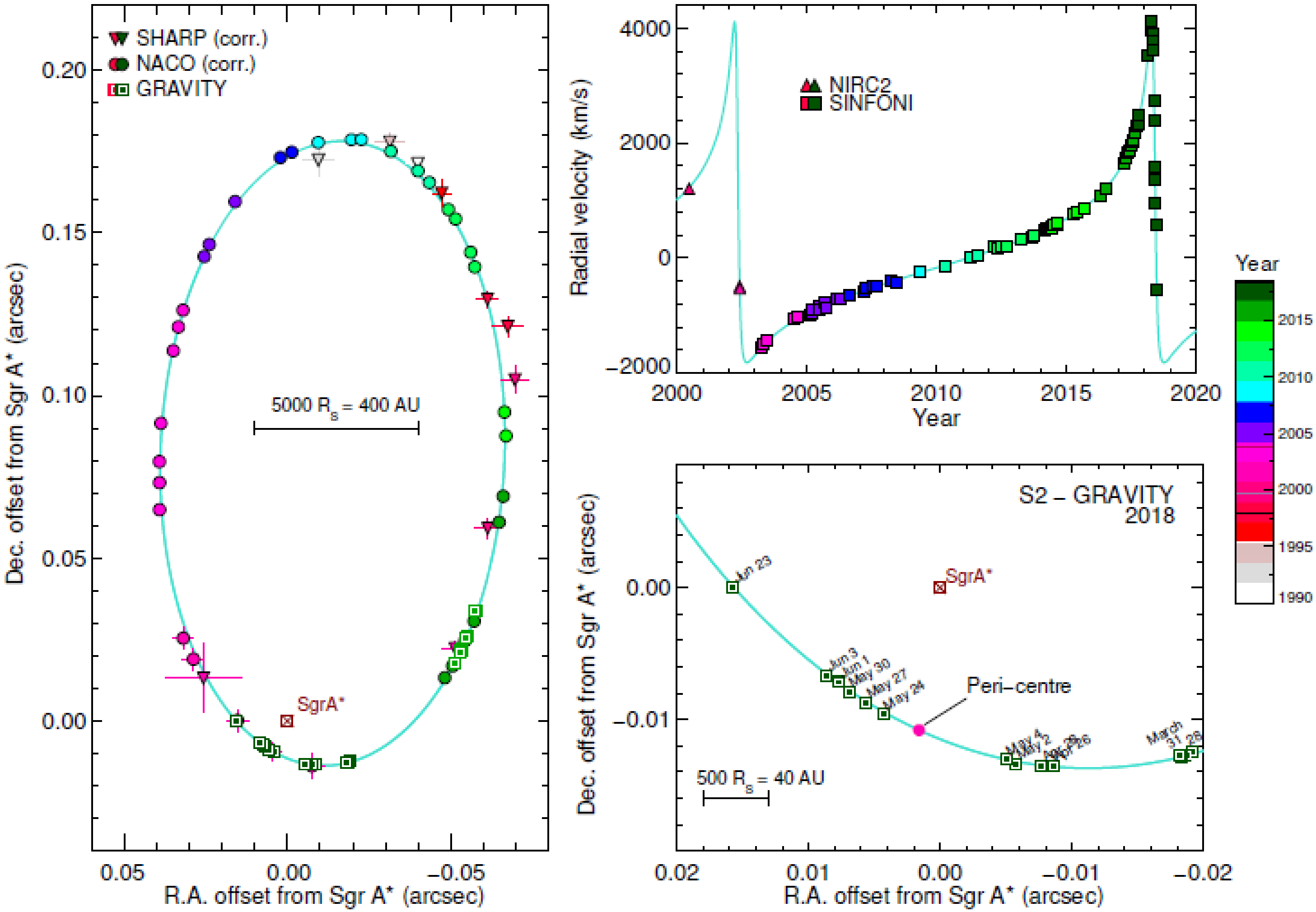

The S2 orbit from 1992 to 2018.

SHARP @ NTT – NACO & SINFONI @ VLT – GRAVITY @ VLTI

Observed Gravitational Redshift

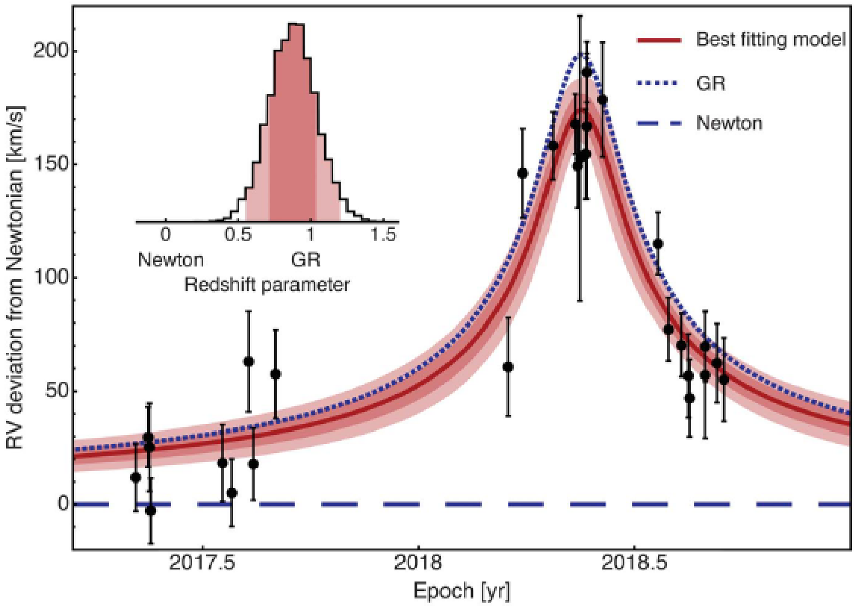

Do, Hees, Ghez et al. 2019, Sci 365, 664

Residual velocity for the best fitting Keplerian and relativistic orbit

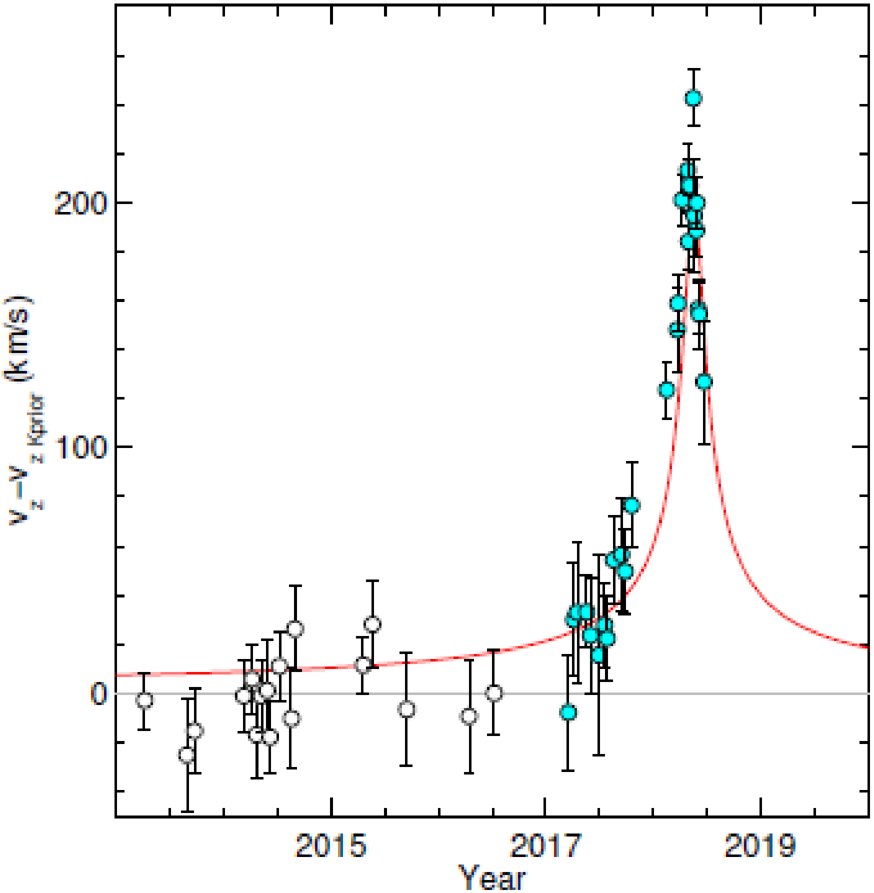

Gravity collaboration 2018, A&A 615, L15

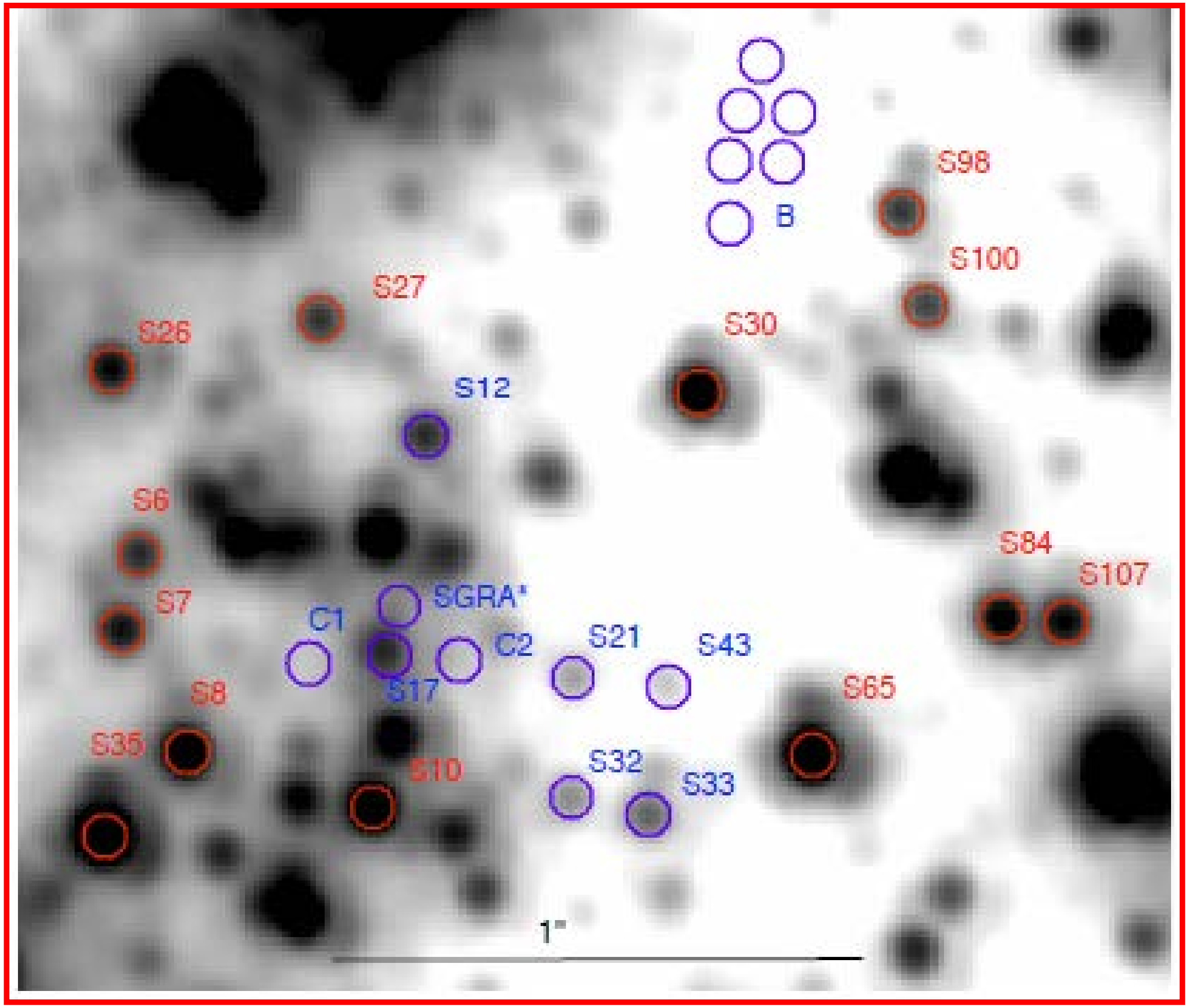

Measurements at 2 μm

Apertures on
(1) SgrA*.
(2) reference stars,
(3) and off-positions

Ks-band mosaic from 2004 September 30. The red circles mark the constant stars (Rafelski et al. 2007) which have been used as calibrators, blue the position of photometric measurements of Sgr A*, comparison stars and comparison apertures for background estimation (Witzel et al. 2012).

Witzel et al. 2012

NIR light curve of SgrA* over 7 years

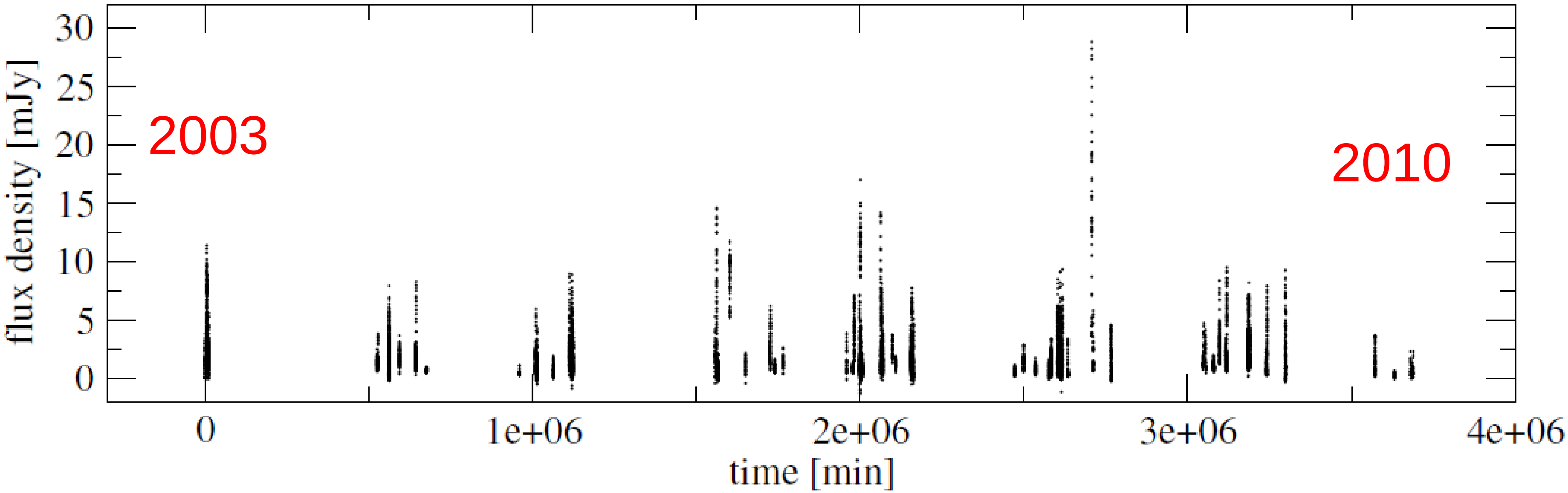

Light curve of Sgr A*. Here no time gaps have been removed, the data is shown in its true time coverage. A comparison of both plots shows: only about 0.4% of the 7 years have been covered by observations.

Witzel et al. 2012

Flux density histogram for SgrA*

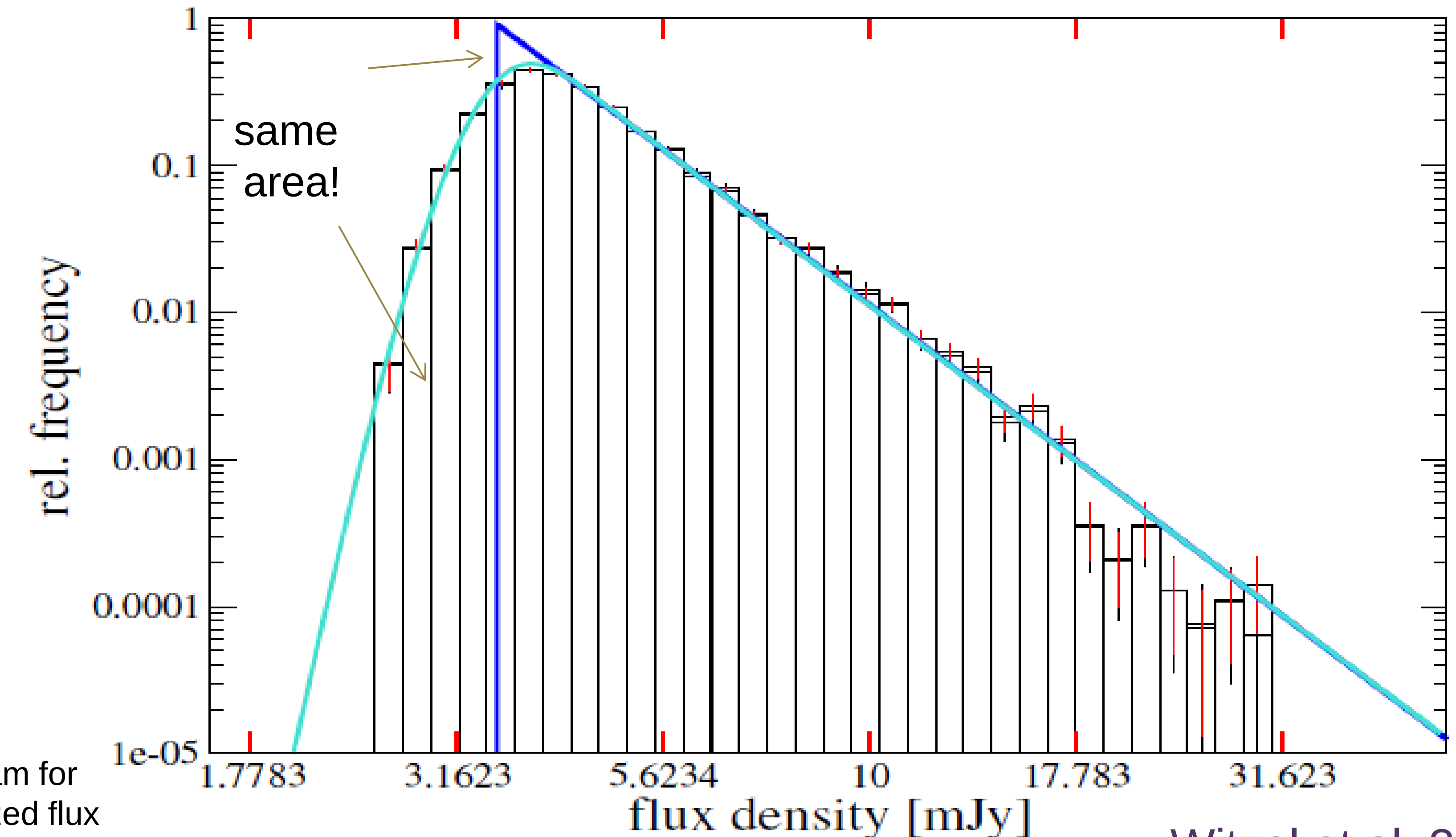

Diagram for polarized flux in work

Witzel et al. 2012

The brown line shows the extrapolation of the best power-law fit, the cyan line the power-law convolved with a Gaussian distribution with 0.32 mJy width.

The statistics allows to explain the event 400 years ago that results in the observed X-ray light echo

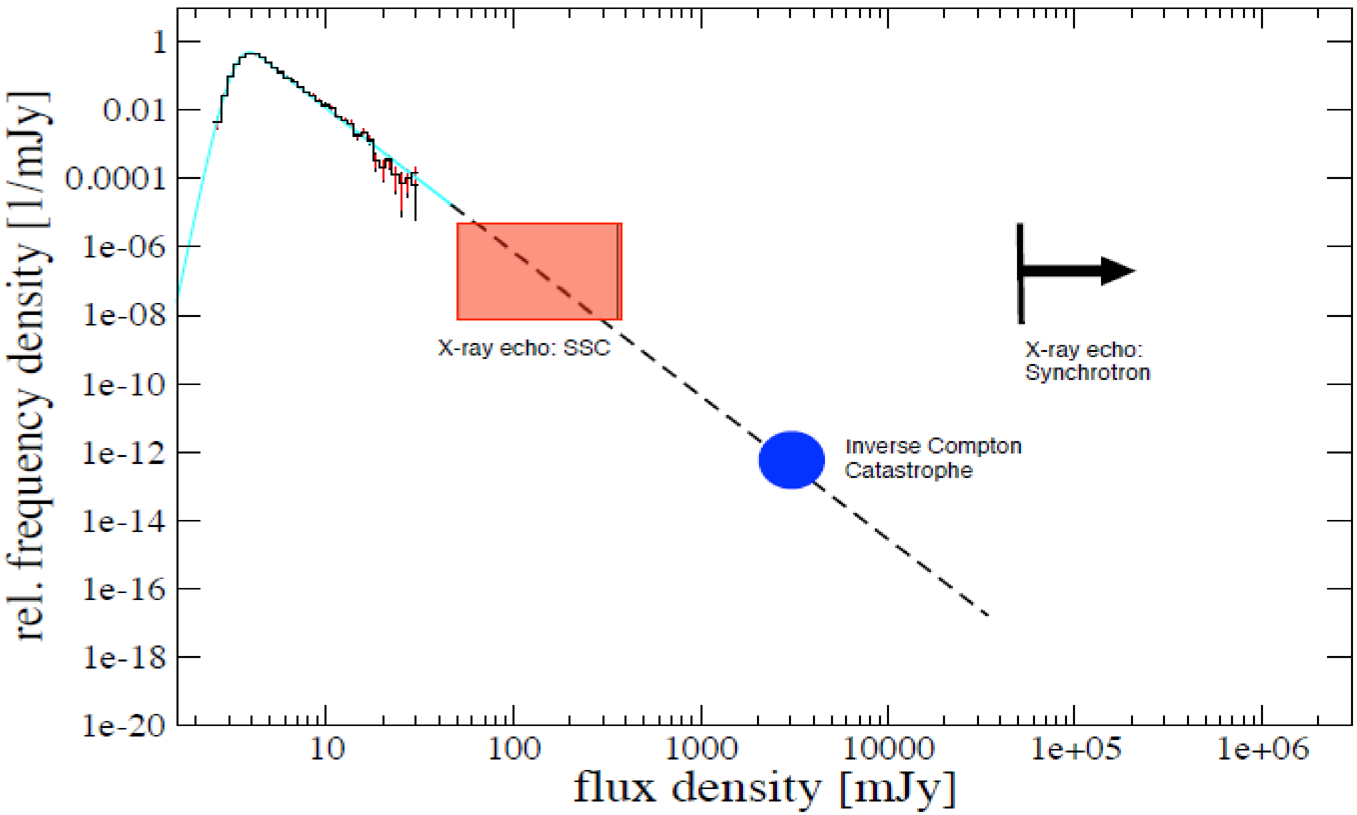

Fluorescent back-scatter from molecular clouds surrounding the GC:

Revnivtsev et al. 2004,
Sunyaev & Churazov 1998,
Terrier et al. 2010

and

Witzel et al. 2012

Illustration of a flux density histogram extrapolated from the statistics of the observed variability. The expected maximum flux density given by the inverse Compton catastrophe and a estimation of its uncertainty is shown
as the magenta circle, the SSC infrared flux density for a bright X-ray outburst as expected from the observed X-ray echo is depicted as the red rectangular.

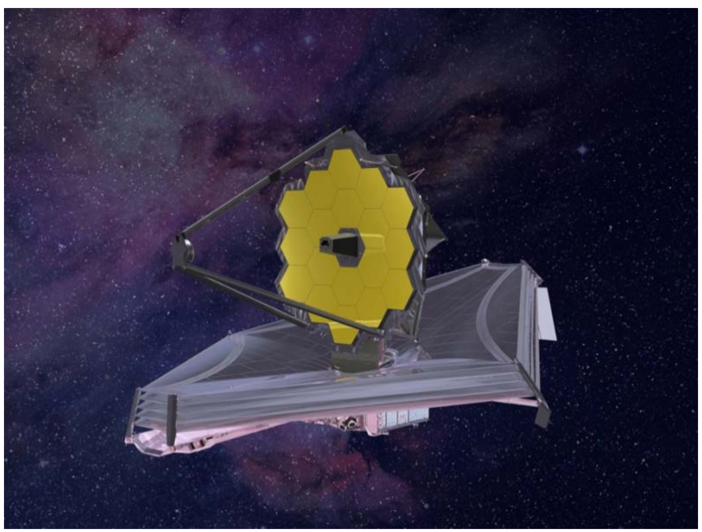

ELT: deeper star count
till main sequence
(stellar population studies)

Larger number of more precise
proper motions and orbits.

Stellar dynamics of central cluster

More high velocity stars
Better probes of relativity

Faint flux density variability of
stars and SgrA*

End